

Contents lists available at SciVerse ScienceDirect

Progress in Biophysics and Molecular Biology

journal homepage: www.elsevier.com/locate/pbiomolbio



Review

Metabolic regulation of the squid nerve Na⁺/Ca²⁺ exchanger: Recent kinetic, biochemical and structural developments

Graciela Berberián^a, Alberto Podjarny^b, Reinaldo DiPolo^{c,*}, Luis Beaugé^{a,**}

- a Laboratorio de Biofísica, Instituto de Investigación Médica "Mercedes y Martín Ferreyra" (INIMEC-CONICET), Casilla de Correo 389, 5000 Córdoba, Argentina
- ^b Department of Structural Biology and Genomics, IGBMC, CNRS, INSERM, Université de Strasbourg, Illkirch, France
- ^cLaboratorio de Fisiología Celular, Instituto Venezolano de Investigaciones Científicas, Apartado 21287, Caracas 1020A, Venezuela

ARTICLE INFO

Article history: Available online 22 September 2011

Keywords: Na⁺/Ca²⁺ exchanger Squid nerve Metabolic regulation Regulatory protein Lipid binding protein Structure—function

ABSTRACT

The Na⁺/Ca²⁺ exchangers are structural membrane proteins, essential for the extrusion of Ca²⁺ from most animal cells. Apart from the transport sites, they have several interacting ionic and metabolic sites located at the intracellular loop of the exchanger protein. One of these, the intracellular Ca²⁺ regulatory sites, are essential and must be occupied by Ca²⁺ to allow any type of ion (Na⁺ or Ca²⁺) translocation. Intracellular protons and Na⁺ are inhibitory by reducing the affinity of the regulatory sites for Ca²⁺; MgATP stimulates by antagonizing H⁺ and Na⁺. We have proposed a kinetic scheme to explain all ionic and metabolic regulation of the squid nerve Na⁺/Ca²⁺ exchanger. This model uniquely accounts for most of the new kinetic data provided here; however, none of the existing models can explain the trans effects of the Ca²⁺-regulatory sites on external cation transport sites; i.e. all models are incomplete. MgATP up-regulation of the squid Na⁺/Ca²⁺ exchanger requires a cytosolic protein, which has been recently identified as a member of the lipocalin super family of Lipid Binding Proteins (LBP or FABP) of 132 amino acids (ReP1-NCXSQ, access to GenBank EU981897). This protein was cloned, expressed and purified. To be active, ReP1-NCXSQ must be phosphorylated from MgATP by a kinase present in the plasma membrane. Phosphorylated ReP1-NCXSO can stimulate the exchanger in the absence of ATP. Experiments with proteoliposomes proved that this up-regulation can take place just with the lipid membrane and the exchanger protein. The structure of ReP1-NCXSQ predicted from the amino acid sequence has been confirmed by X-ray crystal analysis; it has a "barrel" formed by ten beta sheets and two alpha helices, with a lipid coordinated by hydrogen bonds with Arg 126 and Tyr 128.

© 2011 Elsevier Ltd. All rights reserved.

Contents

1.	Introd	duction. Ionic and metabolic regulation of the squid nerve Na ⁺ /Ca ²⁺ exchanger	. 48
2.	New	steady state kinetic analysissteady state kinetic analysis	. 50
	2.1.	Effects of [Na ⁺] _i on Ca ²⁺ influx and on the Ca ²⁺ -stimulated Na ⁺ efflux (reverse exchange) at pH 7.0 in the absence and presence of MgATP	. 50
		2.1.1. Experimental data on the effects of $[Na^+]_i$ on Ca^{2+} influx in the absence of external Na^+	. 50
		2.1.2. Experimental data on the effects of $[Na^+]_i$ on the external Ca^{2+} -dependent Na^+ efflux	. 50
		2.1.3. Simulation data	
	2.2.	Effects of the state of the Ca ₁ ²⁺ -regulatory sites on the apparent affinities of the internal transporting sites	. 51
	2.3.	Unaccounted data on trans effects of the Ca ²⁺ -regulatory sites	. 52
3.	Recen	nt data on metabolic regulation	. 54
	3.1.	The first evidences	. 54
	3.2.	Identification of SCRP	. 55
	3.3.	Functional and biochemical characterization of the recombinant ReP1-NCXSQ	. 55
	3.4.	Metabolic regulation in the squid nerve Na ⁺ /Ca ²⁺ exchanger expressed in alien systems	. 56
		3.4.1. Expression in frog oocytes	. 57
		3.4.2. Expression in yeast	. 58

E-mail addresses: rdipolo@gmail.com (R. DiPolo), lbeauge@immf.uncor.edu, lbeauge@gmail.com (L. Beaugé).

^{*} Corresponding author. Tel.: +58 212 5041230; fax: +58 212 5041093.

^{**} Corresponding author. Tel.: +54 351 4681464; fax: +54 351 4695163.

3.5. Possible pathways involved in the ReP1-NCXSQ dependent metabolic regulation of squid Na ⁺ /Ca ²⁺ exchanger	. 59
Structure of ReP1-NCXSQ	
4.1. Spectral analysis	
4.2. Predicted and solved crystal structure of ReP1-NCXSQ	
Concluding remarks. Comparison with other systems	
Acknowledgments	
References	

1. Introduction. Ionic and metabolic regulation of the squid nerve Na^+/Ca^{2+} exchanger

The Na⁺/Ca²⁺ exchanger is a constitutive plasma membrane protein which, as a major factor for [Ca²⁺]_i clearance (forward Na⁺/Ca²⁺ exchange in Fig. 1), is involved in several cellular processes including cardiac relaxation and neurosecretion (Brinley and Mullins, 1967; Blaustein, 1977a; Matsuda et al., 1997; Bers, 1999; Blaustein and Lederer, 1999; Hurtado et al., 2002; Murphy et al., 2002: Noble, 2002: Romero-Martin et al., 2003: DiPolo and Beaugé, 2006: Cuomo et al., 2008: Formisano et al., 2008: Molinaro et al., 2008; Boscia et al., 2009). In addition to the transporting sites, there are non-transporting Ca²⁺ regulatory regions located on the large intracellular loop (see Hilge et al., 2007). This exchanger is highly regulated by transported and non-transported intracellular ions, as well as by the metabolic state of the cell estimated from the levels of [ATP] (Brinley and Mullins, 1967; Bers, 1999; Blaustein and Lederer, 1999; DiPolo and Beaugé, 2006); most of these regulatory processes occur at the large intracellular loop, disappearing following its deletion (Hilgemann, 1990; Matsuoka et al., 1993; He et al., 1998). In the past few years, our laboratories have developed an integrated kinetic model for MgATP modulation of the squid Na⁺/Ca²⁺ exchanger on the basis of Na_i⁺, H_i⁺ and Ca_i²⁺ interactions with the Cai-regulatory sites and the way they are affected by MgATP (DiPolo and Beaugé, 2006).

All living cells are exposed to an external environment that is chemically and biochemically completely different from the cytosol; this is true for both uni- and multicellular organisms. Two relevant examples can be drawn from our present knowledge, mainly of highly organized species: extracellular [Na⁺] and

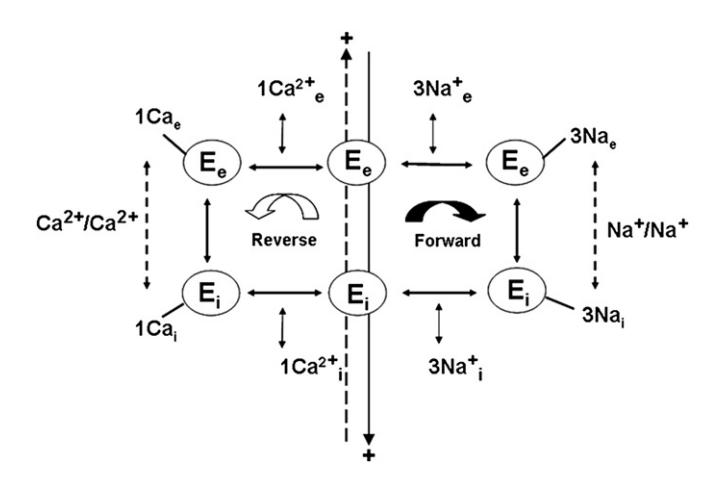


Fig. 1. Different transport modes that occur through the Na $^+$ /Ca $^{2+}$ exchanger. In the cartoon, E represents the exchanger with the extracellular cation transporting sites phasing upward (E $_e$) and the cytosolic downward (E $_i$). The forward Na $_e^+$ /Ca $_i^{2+}$ exchange is indicated by the black curved arrow and the reverse Ca $_e^{2+}$ /Na $_i^+$ exchange by the white curved arrow. Their electrogenic behavior is illustrated by the full and dashed arrows in the center of the figure. The electroneutral Ca $_i^{2+}$ /Ca $_i^{2+}$ and Na $_i^{4+}$ /Na $_e^{4-}$ exchanges are shown by the vertical dashed arrows on the left and right respectively.

[Ca²⁺], and particularly the latter, are much higher in the external media. The cell interior, being electronegative with respect to the exterior, is subjected to large electrochemical gradients favoring net Na⁺ and Ca²⁺ gain. There are two important aspects of this situation: (i) On the one hand, the cells must expend energy to maintain internal homeostasis (an example is Na⁺ extrusion by the Na⁺/K⁺ pump). (ii) On the other, they use some of these gradients to their advantage. For instance, the large electrochemical gradient for Na⁺ permits the uptake of substrates (sugar, amino acids and neurotransmitters, among others) and the extrusion of Ca²⁺ by specific co- and counter-transporters, and the transmission of electrical signals by the generation of action potentials. The Ca²⁺ gradient is used to temporarily raise the concentration of that cation, letting it act as one of the most powerful cell signals.

The Na^+/Ca^{2+} exchange is both electrogenic (1 Ca^{2+} in exchange for 3 Na⁺) and reversible; this means that, depending on the concentrations of the transported ligands, their relative affinities for the transporting sites and the membrane potential, it can produce Ca²⁺ extrusion, together with a net Na⁺ gain, or a net Ca²⁺ gain coupled to the extrusion of Na⁺. There are two other modes of exchange also requiring Ca²⁺ at the regulatory sites: the Na_i⁺/Na_o⁺ and the Ca_1^{2+}/Ca_0^{2+} exchanges; in these modes there is no net transfer of charges, and they are therefore electroneutral. In addition, when a transported species, either Na⁺ or Ca²⁺, is present on one side of the membrane only (inside or outside of the cell) the exchanger runs for a half cycle and then stops; in other words, there is no uncoupled transport. This makes the system highly efficient since it does not produce "leak" fluxes. The four modes of transport are illustrated in Fig. 1. It must be emphasized that the Na⁺/Na⁺ exchange is extremely important as a tool to study the regulatory Ca²⁺ sites without interference when loading the Ca²⁺ transporting sites (see below).

Different models have been proposed to account for the behavior and kinetic properties of the Na⁺/Ca²⁺ exchanger; in mammals the model put forward for the cardiac NCX1 gained wide acceptance (Hilgemann et al., 1992a,b; Matsuoka and Hilgemann, 1992; Hilgemann, 1996; Matsuoka et al., 1996). In these schemes the notion appears for the first time of intracellular Na⁺ inactivation, an inhibition of both pre-steady and steady state exchange currents by Na_i⁺. According to this idea, when the carrier binds Na⁺ to the intracellular transport sites, two competing routes can be followed: transporting Na+ to the outside or shifting into an intracellular inactive state (Ii3Nai). This effect is antagonized by intracellular Ca²⁺, cytosolic alkalinization and MgATP. A similar model, but considering a consecutive 4 Na⁺/1 Ca²⁺ exchange cycle and two inactive states, has also been put forward (Fujioka et al., 2000). These consecutive exchange cycles can explain several of the exchange currents observed in whole cell and in giant membrane patches and intact myocytes. Based on analysis with that kinetic model, it was found that ionic regulation differs in kidney, brain and cardiac muscle NCX isoforms. The main finding was that they show considerable variability in Na_i⁺-inactivation and in the effects of regulatory Ca²⁺, particularly during pulses of changing [Na $^+$]_i, and also in the activation by PKA (Hryshko, 2002; Schulze et al., 2002). It was suggested that a different kinetics of ionic regulation in distinct exchangers is a functional adaptation to the tissue requirements for Ca $^{1+}_1$ regulation.

A different mechanism for H_i^+ protons and $(H^+ + Na^+)$ inhibition of cardiac NCX1 was put forward by Doering and Lederer (Doering and Lederer, 1993, 1994; Doering et al., 1996). In this case Na_i^+ -inactivation is due to a Na^+ enhancement of proton inhibition $(Na^+ - H^+$ synergism) with the sodium-bound forms of the NCX1 having a higher affinity for inhibitory protons than the sodium-free form. This effect does not involve H_i^+ competition at the calcium and sodium translocation sites nor does it take into account the Ca_i^{2+} -regulatory site.

The model we have proposed to explain the activity and kinetics of the Na $^+$ /Ca $^{2+}$ exchange in the squid giant axon focuses on the fact that, in the axon under internal dialysis, it is possible to measure the overall affinity of the intracellular calcium regulatory sites through the Ca $_1^{2+}$ stimulation of the electroneutral Na $_1$ /Na $_0$ exchange, following the effects of different ionic (Na $_1^+$, H $_1^+$ and Ca $_1^{2+}$) and metabolic (MgATP) ligands acting on the regulation of this transporter.

Fig. 2 depicts the integrated kinetic model proposed by us to account for the ionic and MgATP-dependent regulation of the squid nerve Na⁺/Ca²⁺ exchanger. These regulations are based on their influence on the ability of Ca²⁺ ions to bind to its intracellular regulatory sites. The squid axon has a diameter (more than 0.5 mm) that allows a capillary with a limited region of high porosity (molecular weight cut off of 18 kDa) to be introduced. In turn, that permits a uniquely accurate control of the cytosolic ionic and biochemical (substrates and/or products) components of these nerve cells. This procedure, known as internal dialysis, initially developed by Brinley and Mullins (1967) and later improved by us, made it possible to run concentration dependent curves for all intracellular, and obviously extracellular, ligands involved. In addition, it allows the efflux and influx of [⁴⁵Ca]Ca²⁺

to be measured consecutively in the same axon, enabling direct estimation of net Ca²⁺ movements across the membrane. The proposed kinetic model of Fig. 2 predicts that, due to the different affinities of the regulatory intracellular loop sites and transport sites (DiPolo and Beaugé, 2006), one should be able, in principle, to separate ionic regulatory loop sites from Na and Ca transport sites located at the transmembrane segments of the exchanger (Philipson and Nicoll, 2000). This is particularly true when experimental conditions are such that the regulatory Ca²⁺ sites are saturated ($K_{0.5}$ below 1 μ M) while Ca₁²⁺ transport sites, with the $K_{0.5}$ about or greater than 100 μ M Ca²⁺, are far from saturation. The role of the Ca_i^{2+} -regulatory sites in Na_i^+ - H_i^+ -ATP interactions was explored by measuring the Na_0^+ -dependent ⁴⁵Ca²⁺ efflux (Na₀⁺/Ca₁²⁺ exchange) and Ca₁²⁺-dependent ²²Na⁺ efflux (Na₀⁺/Na_i⁺ exchange). The experimental results (see DiPolo and Beaugé, 2006) showed: (i) without ATP, inhibition by Na; is strongly dependent on H_i⁺. Lowering the pH_i 0.4 units from the physiological value of 7.3 causes 80% inhibition of Na₀⁺/Ca₁²⁺ exchange. (ii) In the presence of MgATP, H_i⁺ and Na_i⁺ inhibition is markedly diminished. (iii) Experiments on Na₀⁺/Na_i⁺ exchange indicate that drastic changes in Nai+Hi-ATP interactions take place at the Ca₁²⁺ regulatory sites. The increase in Ca₁²⁺ affinity induced by ATP at pH 6.9 can be mimicked by a rise in pHi from 6.9 to 7.3 in the absence of the nucleotide. Consequently, MgATP modulation of the Na⁺/Ca²⁺ exchange occurs by protection of that site from intracellular proton and sodium inhibition.

Perhaps one of the greatest advantages of the present measurement of the four modes of operation of the exchanger using intracellular dialysis preparation is that the activation of the electroneutral Na_i^+/Na_0^+ exchange by $[Na^+]_i$ depends only on the binding of Ca^{2+} to its regulatory intracellular loop site and therefore allows real measurement of the affinity of the Ca_i^{2+} -regulatory site. This is not possible with all other modes of translocation of the exchanger $(Na_0^+/Ca_i^{2+},Ca_i^{2+}/Na_0^+$ and $Ca_i^{2+}/Ca_0^{2+})$, since Ca^{2+} ions are involved in the translocation pathway.

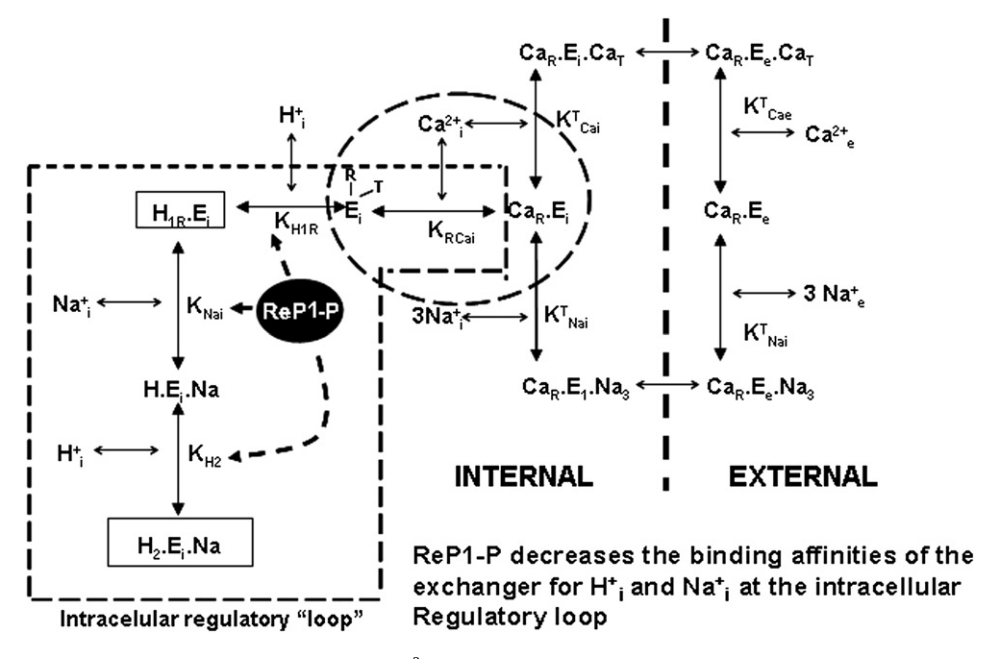


Fig. 2. Reaction scheme for transport and regulation of the squid nerve Na^+/Ca^{2+} exchange. The overall translocation cycle is represented by the arrows linking the complexes of the carrier bound to Ca^{2+} at the regulatory site $(Ca_R \cdot E)$ with those binding Ca^{2+} $(Ca_R \cdot E \cdot Ca_T)$ and Na^+ $(Ca_R \cdot ENa_T)$ at the intra- and extracellular transport sites. The intra- and extracellular environments are separated by a thick dashed vertical line. The dashed oval defines the reaction leading to the binding of Ca^{2+} to its intracellular regulatory sites. The dashed line on the left schematizes the intracellular regulatory loop with the sites for H_i^+ and $H_i^+ + Na_i^+$ synergic inhibitions together with the release of those inhibitions by phosphorylated ReP1-NCXSQ (ReP1-P). The dissociation constants for the complex interconversions are self explanatory and represent the ratio of "off" and "on" binding constants given in Beaugé and DiPolo (2008). Simulations were conducted by using these unidirectional constants. Redrawn from Beaugé and DiPolo (2008) with permission.

These findings are all predicted by a model in which: (i) The binding of Ca^{2+} to the regulatory sites is essential for translocation but not for the binding of Na_i^+ or Ca_i^{2+} to the transporting site; (ii) H_i^+ competes with Ca_i^{2+} for the same form of the exchanger without affecting that of the Ca_i^{2+} transporting site; (iii) protonation of the carrier (pH $_i$ > 7.4) increases the apparent affinity of the exchanger by changing cooperativity for Na_i^+ binding at the Na_i^+ inhibitory site; (iv) ATP prevents both H_i^+ and Na_i^+ effects. These recent developments in ionic and metabolic regulation of the squid nerve Na^+/Ca^{2+} exchanger are the topics of this review.

2. New steady state kinetic analysis

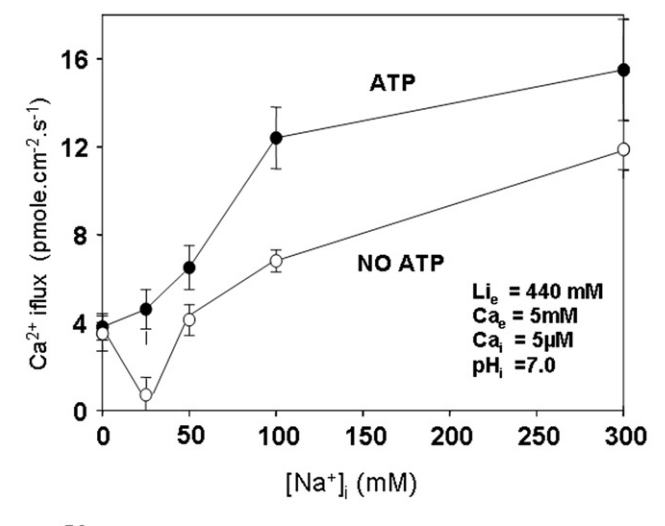
2.1. Effects of $[Na^+]_i$ on Ca^{2+} influx and on the Ca_e^{2+} -stimulated Na^+ efflux (reverse exchange) at pH 7.0 in the absence and presence of MgATP

The kinetic scheme for the squid Na⁺/Ca²⁺ exchanger in Fig. 2 indicates that intracellular Ca²⁺ will always counteract H_i⁺ and Na_i⁺ inhibition. The reason is that, following its binding to the regulatory sites (Ca_RE_i), it will take the cycle away from the inhibitory loop by forming the intracellular Ca²⁺ transporting intermediate Ca_RE_i·Ca_T. The situation is quite different with internal Na⁺ because this cation can take the exchanger into two opposite routes: by binding to its inhibitory site it will force the system into the dead end H₂·E_i·Na complex, while by forming the intracellular Na^+ transporting intermediate $Ca_R \cdot E_i \cdot Na_3$ it will pull the system away from the $(H_i^+ + Na_i^+)$ synergic inhibition path. Which one will prevail will depend on the relative Na⁺ affinities for both routes: and during steady state flux measurements the results will also depend on what cation flux is being measured. The experimental design used in these studies on dialyzed axon consisted of: (i) facilitation of Na_i⁺ inhibition was acquired with internal acidification to pH_i 7.0 in the absence of MgATP; (ii) internal [Na⁺] varied from zero to 300 mM; (iii) the synergic $(H_i + Na_i^+)$ inhibition was antagonized by addition of 3 mM MgATP; (iv) the external solution contained no Na⁺, this cation being replaced with Li⁺; Finally, (v) two fluxes were estimated, the influx of Ca^{2+} and the Ca_e^{2+} dependent efflux of Na⁺ (Beaugé and DiPolo, 2008).

2.1.1. Experimental data on the effects of $[Na^+]_i$ on Ca^{2+} influx in the absence of external Na^+

The top of Fig. 3 summarizes a series of experiments on the influx of [45 Ca]Ca $^{2+}$, where the concentration of this cation was 5 μ M on the inside and 5 mM on the external solution. In the absence of Na_i the uptake of Ca²⁺ represents an electroneutral Ca²⁺/Ca²⁺ exchange mode. As [Na⁺]_i is increased in the absence of MgATP, a dual effect of Nai⁺ becomes evident: inhibition at low [Na⁺]_i followed by activation at higher [Na⁺]_i. When 3 mM MgATP was added to the dialysis medium. Na; inhibition is not present, being replaced by a sigmoid stimulation of the Ca²⁺ influx. In other words, MgATP completely overcomes the dual effect of Nai on Ca2+ influx. These results are completely in line with the predictions of the model outlined above. Without MgATP, internal sodium ions drive the exchanger into two opposite conformations: at low concentrations [Na_i⁺] the formation of the dead end H₂E_iNa complex prevails, and as [Na⁺]_i increases, the Ca_RE_iNa₃ complex comes into play, extruding Na⁺ in exchange for extracellular Ca²⁺. At this stage, the original Ca²⁺/Ca²⁺ exchange is replaced by a Na_i⁺/Ca_e²⁺ reversal exchange. What MgATP actually does is, by reducing the affinity of the inhibitory sites for H_i⁺ and Na_i⁺, it directs.

 ${
m Na}^+$ into the ${
m Na}^+$ extruding branch of the cycle. Other experiments (not shown here) demonstrate that, under similar conditions, internal ${
m Na}^+$ monotonically inhibits the efflux of ${
m Ca}^{2+}$ more effectively in the absence than in the presence of MgATP.



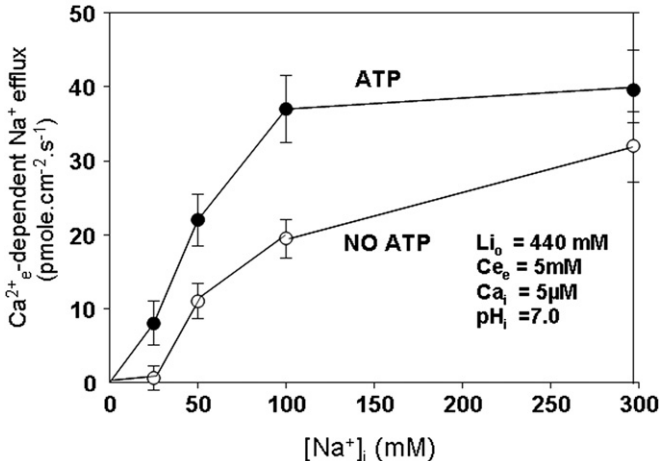


Fig. 3. Top: Effects of $[Na^+]_i$ on $[^{45}Ca]Ca^{2+}$ influx in squid giant axons dialyzed at pH_i 7.0 in the absence and presence of MgATP. Ordinate: Ca^{2+} influx, in pmol cm⁻² s⁻¹ Abscissa: Time in minutes. Note: (i) All extracellular solutions were Na+-free; (ii) Ca2+ influx at 5 $\mu M~Ca_i^{2+}$ (in the absence of intracellular Na^+ starts in the Ca_i^{2+}/Ca_i^{2+} exchange mode); (iii) in the absence of MgATP (open circles) the influx of Ca2+ is inhibited by 25 mM Nai⁺ and is then progressively activated upon increasing [Na⁺]_i to 50, 100 and 300 mM, surpassing the Ca_e^{2+}/Ca_e^{2+} exchange values; (iv) in the presence of 3 mM MgATP (filled circles) there is no Na_i^+ inhibition of Ca^{2+} influx but, in contrast, it is monotonically stimulated by Na_i^+ . The points represent mean \pm SEM of four and five axons respectively. The ionic composition of the intracellular solution is indicated in the figures. Bottom: Effects of $[Na^+]_i$ on Ca_e^{2+} -stimulated $[^{22}Na]Na^+$ efflux (reverse Na⁺/Ca²⁺ exchange) in squid giant axons dialyzed at pH_i 7.0 in the absence and presence of MgATP. Ordinate: Ca₀-dependent Na⁺ efflux in pmol cm⁻² s⁻¹. Abscissa: [Na+]i in mM. Note: (i) the external solutions were Na+-free; (ii) intracellular Na+ stimulates the Ca_0 -dependent Na^+ efflux through a sigmoid curve; (iii) the $K_{1/2}$ for Na_1^+ activation is about 80 mM in the absence (open symbols) and 37 mM in the presence (filled symbols) of 3 mM MgATP. The points represent mean \pm SEM (n=3). Partial reproduction from Beaugé and DiPolo (2008) with permission.

2.1.2. Experimental data on the effects of $[Na^+]_i$ on the external Ca^{2+} -dependent Na^+ efflux

The bottom of Fig. 3 describes experiments on Ca₁²⁺-dependent Na⁺ efflux (reversal exchange) as a function of [Na⁺]_i performed under conditions identical to those for Ca²⁺ influx (shown in Fig. 3A). Actually, these data constitute an excellent complement of those seen at the top of the figure. In the absence of MgATP, 25 mM Na_i⁺ has no effect whatsoever on the efflux of Na⁺. This shows that the reduction in Ca²⁺ influx seen above is not replaced by a reversal exchanger; indeed, for all practical purposes, there are no cation fluxes through the Na⁺/Ca²⁺ exchanger. Consequently, it proves that Na⁺ inhibition takes place by sending the exchanger into the

dead end H_2EiNa conformation. As expected, in these experiments higher $[Na^+]_i$ induces the reversal exchange mode. The picture changes in the presence of 3 mM MgATP, where reversal exchange is seen already at 25 mM Na_i^+ . The end result is that the Na_i^+ activation of the reversal exchange mode is more sigmoid in the absence than in the presence of MgATP, with the $K_{0.5}$ for Na_i^+ going from 80 mM to 37 mM respectively.

It is important to point out that the Na⁺/Ca²⁺ exchange fluxes (forward or reverse) are electrogenic and can be followed by electrophysiological methods. However, the relations between intracellular pH, [Na⁺], [Ca²⁺] and MgATP on the dual effect of Na_i⁺ on Ca²⁺ influx could have not been detected by electrophysiology but required analysis of the type obtained by measuring isotopic estimated cation fluxes.

2.1.3. Simulation data

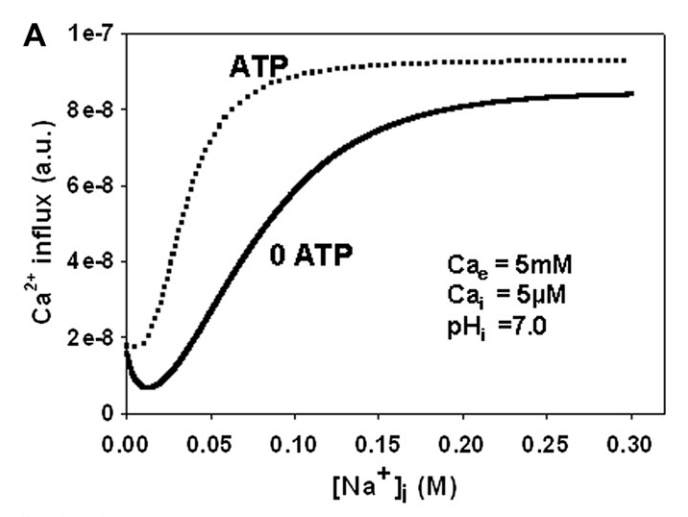
By using the unidirectional rate constants corresponding to the model of Fig. 2 and given in Beaugé and DiPolo (Beaugé and DiPolo, 2008), we simulated the conditions explored in Fig. 3.

The results, depicted in Fig. 4, agree quite well with the above experiments. In Fig. 4A, the dual effect of intracellular Na⁺ on the influx of Ca²⁺, inhibition at low [Na⁺]_i followed by activation at high [Na⁺]_i concentrations, is replaced by a monotonic activation in the presence of 3 mM ATP. We have shown (DiPolo and Beaugé, 2002) that the up-regulation of the exchanger due to MgATP can be mimicked by internal alkalinization. We therefore performed other simulations demonstrating that, at alkaline pH_i, the dual effect of Na_i⁺ on Ca²⁺ influx is not seen even in the absence of ATP. Similar agreement was observed when simulating the Ca_e²⁺-stimulated Na⁺ efflux as a function of intracellular [Na⁺] (Fig. 4B). In addition, on the basis of a value of 3 for the Na⁺ efflux/Ca²⁺ influx ratio, and subtracting the efflux from the influx of Ca²⁺ at the different Na₁⁺ concentrations, we estimated the Na+ efflux in exchange for extracellular Ca²⁺. This gave an apparent affinity for Na_i⁺ of about 100 mM in the absence, and around 30 mM in the presence of MgATP (see DiPolo and Beaugé, 2006).

Another significant finding is that we were unable to predict the dual effects of intracellular Na $^+$ on the influx of Ca $^{2+}$ either with the models proposed by Matsuoka and Hilgemann (Matsuoka and Hilgemann, 1992) or with that suggested by Fujioka et al. (Fujioka et al., 2000) for the mammalian heart Na $^+$ /Ca $^{2+}$ exchanger (NCX1). Obviously this does not mean that those models are wrong. It can very well be that NCX1 and the squid exchanger have indeed different kinetic pathways; at any rate, the experimental and simulation data presented here cannot be accounted for solely in terms of Na ^+_i interactions with the intracellular translocation sites as proposed by the models for NCX1 function. On these points, it would be interesting to explore the effect of internal Na $^+$ on Ca $^{2+}$ influx in a preparation expressing NCX1, keeping in mind that an electrophysiological approach will be of no use in this case.

2.2. Effects of the state of the Ca_i^{2+} -regulatory sites on the apparent affinities of the internal transporting sites

In dialyzed squid axons with the Ca_1^{2+} -regulatory sites saturated, neither MgATP nor pH_i affects the affinity of the intracellular transport sites for Ca^{2+} or Na^+ . And this is independent of the saturating mechanism: high $[Ca^{2+}]_i$ without MgATP at normal pH_i , low $[Ca^{2+}]_i$ with MgATP and normal pH_i or low $[Ca^{2+}]_i$ without MgATP at alkaline pH_i . In addition, those affinities are not affected by protons in the presence of MgATP, or by MgATP at alkaline pH_i (DiPolo and Beaugé, 2008; Beaugé and DiPolo, 2009). On the other hand, at pH_i 7.0 the inhibition of Ca^{2+} efflux by Na_i^+ is more pronounced in the absence than in the presence of MgATP (Beaugé and DiPolo, 2008). With MgATP, that Na_i^+ inhibition represents



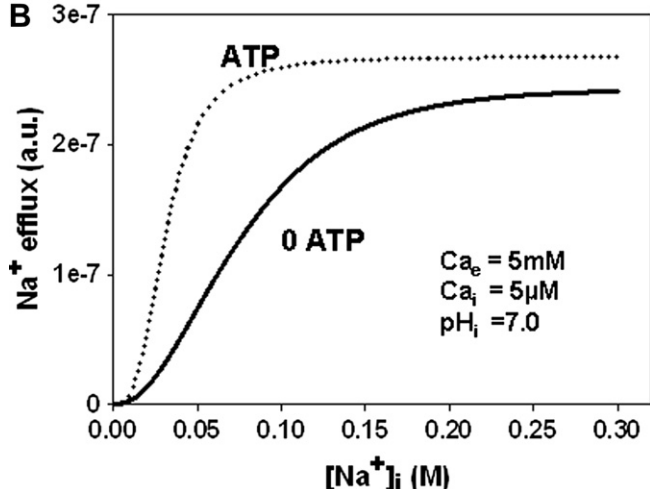


Fig. 4. (A) Model simulation of the effects of intracellular Na⁺ on the influx of Ca²⁺ in an axon with an internal solution containing 5 μ M Ca²⁺, a pH of 7.0 units with and without MgATP. The extracellular solution is Na+-free and contains 5 mM Ca²⁺. Ordinate: Ca²⁺ influx in arbitrary units. Abscissa: [Na⁺]_e in molar. Note: (i) Na_i⁺ inhibition is observed in the absence but not in the presence of ATP; (ii) the simulation adequately reproduces the results shown in Fig. 3 Top. (B) Model simulation of the effects of intracellular Na^+ on Ca_e^{2+} -stimulated [^{22}Na] Na^+ efflux (reverse Na^+ / Ca^{2+} exchange) in squid giant axons dialyzed at pHi 7.0 in the absence and presence of MgATP. The intracellular solution contains 5 μM Ca²⁺, a pH of 7.0 with and without 3 mM MgATP and variable [Na+]; the extracellular medium is free of Na+ and has 5 mM Ca²⁺. Note: (i) intracellular Na⁺ activates the reverse exchange (Ca₀²⁺/Na_i⁺) through a sigmoid curve in both instances; (ii) the apparent affinity for Nai+ is lower in the absence than in the presence of ATP; (iii) the simulation adequately reproduces the results shown at the bottom of Fig. 3. All simulations were carried out with the kinetic model and values given in Beaugé and DiPolo (2008). Taken from Beaugé and DiPolo (2008) with permission.

competition with Ca²⁺ for the internal transporting sites; then, without MgATP, inhibition must have an additional component taking place somewhere else. As the nucleotide does not affect the intrinsic affinities of the intracellular transport sites for Na⁺ or Ca²⁺, other sites, perhaps the Ca²⁺-regulatory ones, are involved.

Encouraged by the results presented in the previous sections, we performed model simulations on the effect of the state of regulatory sites on the *apparent* affinities for internal Na⁺ and Ca²⁺ transporting sites; we stress the word *apparent* because the true affinities were left unmodified. In fact, all basal rate constants remained the same and the changes in the affinity of the regulatory sites were induced either by changes in internal pH or addition of MgATP. These simulations were followed by actual experiments

carried out in dialyzed axons; all the data is presented in Fig. 5, reproduced from (Beaugé and DiPolo, 2009). The effects on the Nai sites were followed by the Ca₁²⁺-dependent Na⁺/Na⁺ exchange; those on Ca₁²⁺ sites by the Na_e⁺-dependent Ca²⁺ efflux; the coincidence between experimental and simulated results is excellent. The apparent affinity of the intracellular transport sites is reduced as the Ca²⁺-regulatory sites become unsaturated, and this is more noticeable, and can be experimentally detected, for Na⁺ but not for Ca²⁺. The reason lies in the two opposite actions of Na_i⁺ and a single effect of Ca_i²⁺. Sodium, on the one hand, inhibits transport by promoting proton binding to the HE₁Na complex and, on the other, activates transport by binding to the uninhibited carrier, inducing Ca_RE_iNa₃ followed by translocation to the extracellular medium. The balance between these two conformations is shifted toward HE_iNa at acidic pH_i (6.9) and to $Ca_RE_iNa_3$ at alkaline pH_i (8.8). Ca^{2+} can only prevent H_i^+ + Na_i^+ synergic inhibition: directly, by competing with H⁺ for E_i and, indirectly, by binding to the Ca_itransporting site, shifting the $Ca_RE_i \leftrightarrow Ca_RE_iCa_T$ equilibrium to the right. The reason for the difficulty in its experimental detection is that the affinity of the $[Ca^{2+}]_i$ transporting sites is much lower (K_m $100-200 \mu M$) compared to that needed to saturate the Ca_i^{2+} regulatory site, even under adverse conditions ($K_{0.5}$ around 20 μ M (DiPolo and Beaugé, 2002, 2008)).

2.3. Unaccounted data on trans effects of the Ca_i^{2+} -regulatory sites

An old and then unexplained observation of the 1970s was that, in dialyzed squid axons, ATP levels affected the affinity for external

Na⁺ in its stimulation of the forward Ca₁²⁺/Na_e⁺ exchange (Baker and Glitsch, 1973; DiPolo, 1974; Baker and McNaughton, 1976; Blaustein, 1977b): depletion of ATP decreased from one half to one third the $K_{0.5}$ for Na_e⁺ as compared with the values seen in axons with normal ATP content; and this occurred without changes in the Hill coefficient (Blaustein, 1977b). Knowing that MgATP up-regulates the Na⁺/Ca²⁺ exchanger through an increase in the affinity of the Ca₁²⁺ regulatory sites, and with the hypothesis that these *trans* effects involved the state of those sites, we recently re-explored the matter (DiPolo and Beaugé, 2008) expanding it to the external Ca²⁺ transporting sites. The external sodium sites were explored by following the forward Na_e⁺-dependent Ca²⁺ efflux and those for Ca²⁺ with the Ca_e²⁺-stimulation of the Ca²⁺/Ca²⁺ exchange mode. The occupancy of the Ca₁²⁺-regulatory sites was modified in several ways by changing [Na⁺]_i, [Ca²⁺]_i, pH_i and depletion-repletion of MgATP

All results concurred in that an increase in the saturation of the Ca_i^{2+} -regulatory site induced an increase in both the external Na^+ and Ca^{2+} affinities while the reverse was the case for a reduction in saturation. Fig. 6 summarizes the results of experiments where variations in occupancy of the Ca_i^{2+} -regulatory sites were obtained by changing $[Ca_i^{2+}]$ at pH_i 7.3 in the absence of Na_i^+ and MgATP.

With these results, the initial data on ATP effects on Na_e^+ affinity, now extended to Ca_e^{2+} transporting sites, can now be associated with the state of the Ca_i^{2+} -regulatory site. However, the intimate mechanism/s was not established. In an attempt to relate them to kinetic effects, we performed simulations with three kinetic models for Na^+/Ca^{2+} exchange: those proposed for mammalian

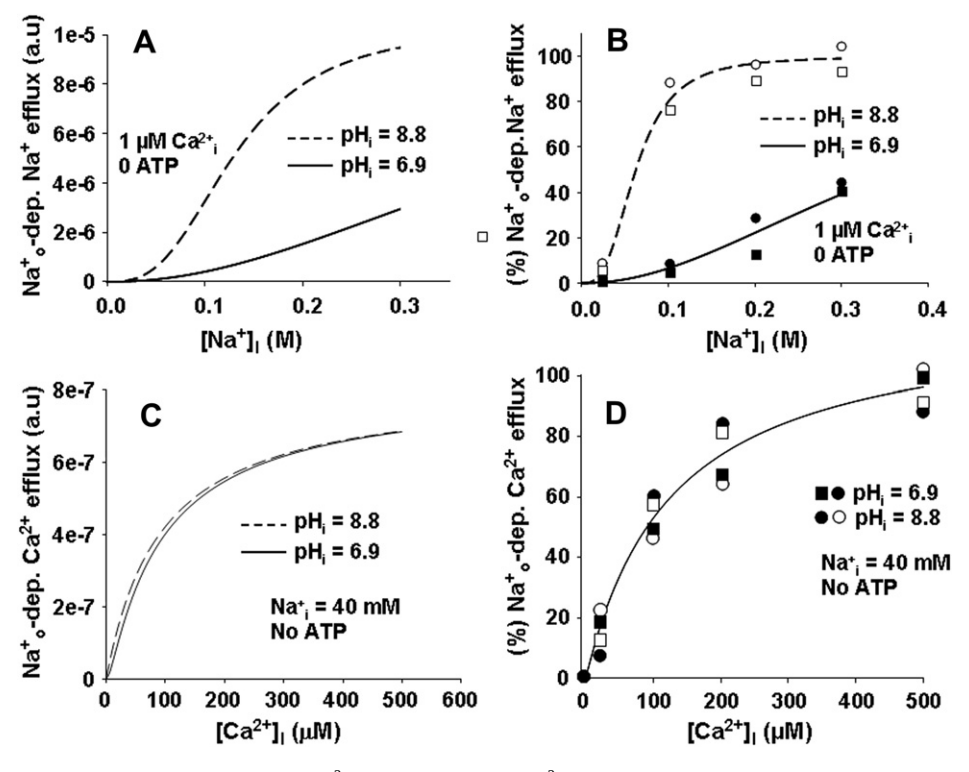


Fig. 5. Top: Na_i^+ -stimulation of Na_o^+/Na_i^+ exchange through the Na^+/Ca^{2^+} exchanger with 1 μM [Ca^{2^+}]_i at acidic and alkaline pH_i. Figure A describes simulation results while Figure B shows the data points of two different experiments in which each axon was subjected to both conditions. They are expressed as a percentage of the maximal flux assuming it was similar for both pH_i's. The lines through the points correspond to the best fit to a Hill equation with the following fit parameters (Mean ± SEM from the fit): pH 6.9: Ks of 343 ± 66 mM and a Hill coefficient of 2.66 ± 0.37. pH 8.8: Ks of 63 ± 35 mM and a Hill coefficient of 3.01 ± 0.33 (P < 0.001). Ordinate: Percentage of $Ca_i^{2^+}$ -dependent Na_o/Na_i exchange. Abscissa: intracellular [Na^+] in mM. The dialysis solutions contained 1 μM Ca^{2^+} , 0.5 mM free Mg^{2^+} and no ATP. The pH's were 6.9 (filled symbols) and 8.8 (open symbols). Bottom: Stimulation by $Ca_i^{2^+}$ of the Na_o^+ -dependent Ca^{2^+} efflux (forward exchange mode) at acidic and alkaline pH_i. Figure C describes simulation data and Figure D shows the results from two different experiments in which the same axon was exposed to different pH_i's. They are expressed as a percentage of the maximal flux assuming it was the same for both pH_i's. The line through the points corresponds to the best fit to a Michaelian function with a Km of 95 ± 6.8 μM (Mean ± SEM from the fit) and was the same for both conditions. Ordinate: Percentage of $Ca_i^{2^+}$ -stimulated $Na_o^{2^+}$ -dependent Ca^{2^+} efflux. Abscissa: intracellular Ca^{2^+} concentration in μM. The dialysis solutions contained 40 mM $Na_o^{2^+}$, 0.5 mM Mg^{2^+} , no ATP, at pH_i 6.9 (filled symbols) and pH_i 8.8 (open symbols). Taken from Beaugé and DiPolo (2008) with permission.

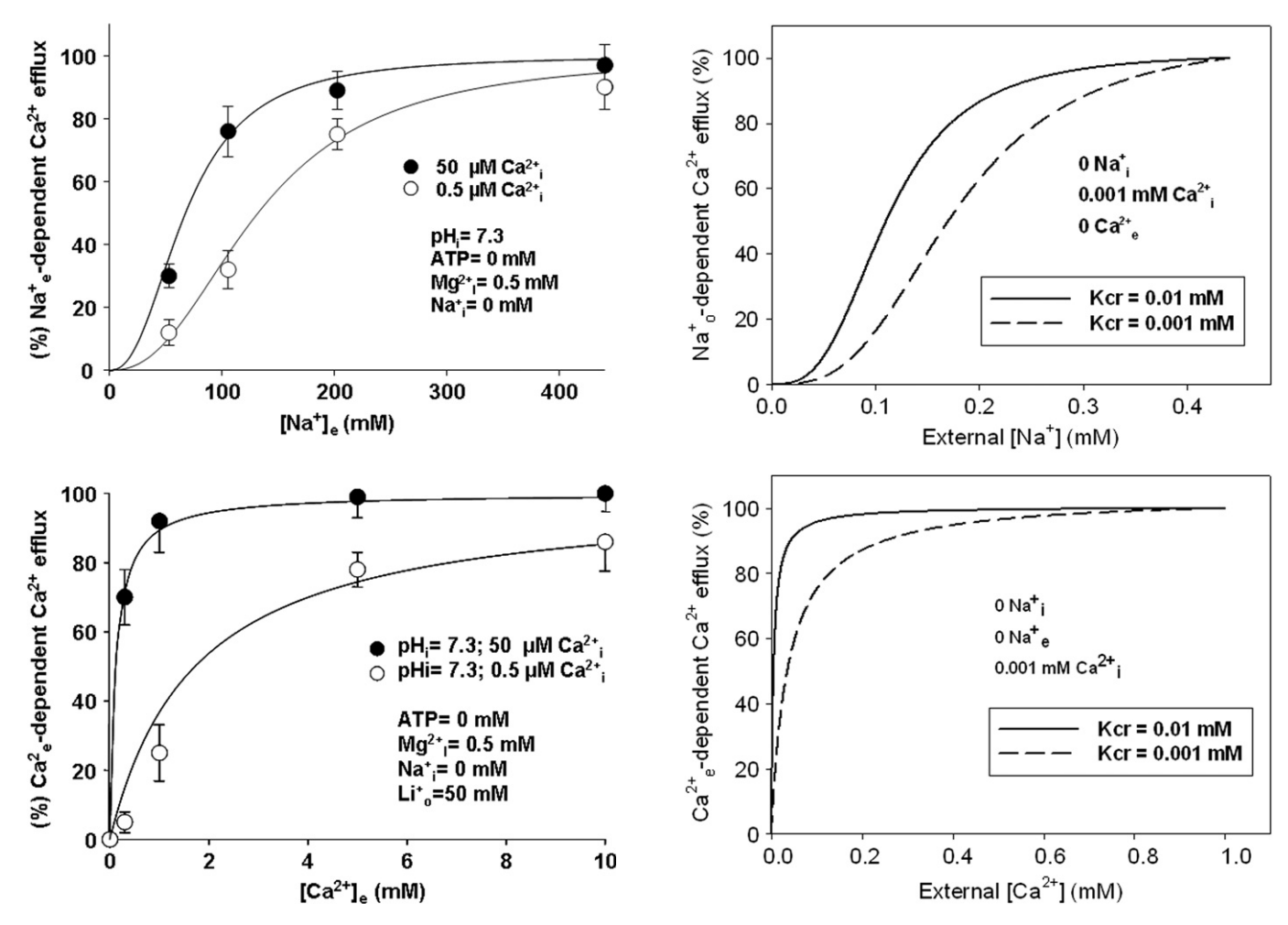


Fig. 6. Experimental data on the effects of the level of activation of the Ca₁²⁺-regulatory sites on the affinity of the external cation transport sites of the squid Na^+/Ca^2 exchanger. Top: External Na $^+$ sites. Normalized data, mean \pm SEM, of three different experiments in which each axon was dialyzed first with 0.5 μM Ca_i²⁺ (open circles, Ca_iregulatory sites unsaturated) and then with 50 μM Ca_i²⁺ (filled circles, Ca_i-regulatory sites saturated). The points express a percentage of the maximal flux estimated from the fit for each condition. The lines through the points correspond to the simultaneous best fit to a Hill equation taking two different Ks and a single Hill coefficient: (a) $0.5\,\mu M$ Ca_i^{2+} : Ks of 132 \pm 8 mM Na⁺; (b) Ks of 68 \pm 6 mM Na⁺. The Hill coefficient had a value of 2.48 \pm 0.18. Ordinate: Percentage of Na_0^+ -dependent Ca^{2+} efflux. Abscissa: extracellular [Na+] in mM. The dialysis solutions contained 0.5 mM free Mg²⁺ and had a pH of 7.3. In addition, they were free of Na_i⁺ and ATP. Note that the affinity for external Na⁺ increases with the saturation of the Ca₁²⁺-regulatory sites. Bottom: External Ca²⁺ sites. Mean + SEM of data from three different experiments in which each axon was dialyzed with 0.5 μM Ca_i^{2+} (open circles: unsaturated Ca_i -regulatory sites) and 50 μM Ca_i^{2+} (filled circles: saturated Cai-regulatory site). The points express the percentage of the maximal flux at each Ca²⁺ concentration. The lines through the points correspond to the simultaneous best fit to a Michaelian function. The estimated Km's from the fit were 0.12 \pm 0.03 mM at 50 μ M Ca_{i}^{2+} and 1.7 \pm 0.3 mM at 0.5 μ M Ca_{i}^{2+} . The dialysis solutions also contained 0.5 mM Mg^{2+} and 50 mM Li $^{+}$ and had a pH of 7.3. In addition, they were free of Na+ and ATP. The extracellular solutions were Na+-free and contained 50 mM Li⁺. Ordinate: Percentage of Ca₀²⁺-dependent Ca²⁺ efflux. Abscissa: extracellular Ca^{2+} in mM. Note that the affinity for external Ca^{2+} increases (P < 0.001) with the saturation of the Ca²⁺-regulatory sites. Taken from Beaugé and DiPolo (2008)

heart (Matsuoka and Hilgemann, 1992; Fujioka et al., 2000) and that suggested by us for the squid nerve.

Fig. 7 shows simulation with the squid nerve kinetic scheme. Very importantly, the results of these simulations were identical to those obtained with the two models for the mammalian heart (Matsuoka and Hilgemann, 1992; Fujioka et al., 2000; personal results not shown here). In other words, all three models predict

Fig. 7. Model simulations of the effects of changes in the saturation of the Ca_1^{2+} regulatory sites on the affinity of the transporting sites of the Na^+/Ca^{2+} exchanger for extracellular Na^+ (top) and Ca^{2+} (bottom). The fluxes were normalized to the maximal flux in each condition. The model used was that proposed for the squid (DiPolo and Beaugé, 2002; Beaugé and DiPolo, 2009) but identical results were obtained with those suggested for the mammalian heart (Matsuoka and Hilgemann, 1992; Fujioka et al., 2000). Note: (i) the simulations predict that when the Ca_1 -regulatory sites is impaired (decrease in saturation) there is an increase in the affinities for the external transporting cations; (ii) this is the opposite of what was found in the squid (Beaugé and DiPolo, 2008) and was not observed in the mammalian heart following ATP depletion (Haworth and Biggs, 1997).

that a decrease in the saturation levels of the Ca²⁺-regulatory sites should lead to an increase in the apparent affinities of the external transporting sites: in other words, the predictions are just the opposite of the observations. Actually, the predictions concur with a system that has "ping-pong" kinetics (Blaustein and Lederer, 1999), an assumption underlying these schemes. We have recently shown that, leaving aside the regulatory loop, the overall transport reaction of the squid exchanger is indeed "ping-pong" (Beaugé and DiPolo, 2009). Interestingly, Haworth and Biggs (1997) found that, in Na⁺ loaded rat heart cells, ATP depletion resulted in an eight-fold reduction in V_{max} for Ca^{2+} uptake (reverse exchange) but produced no significant change in the K_{m} for extracellular Ca^{2+} or the K_{i} for inhibition by extracellular Na⁺. Again, these results cannot come from a system obeying a simple ping-pong mechanism. Interestingly, in the Na⁺/K⁺-Pump, changes in the metabolic state of the cells (ATP levels) have indeed produced evidence for a ping-pong mechanism (Eisner and Richards, 1980). Actually, the concentrations of ATP used were those acting on the nucleotide regulatory

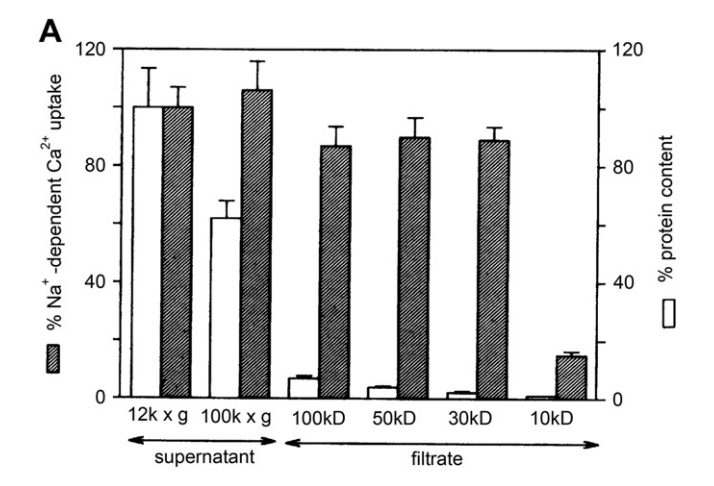
site. However, a direct comparison with the Na $^+$ /Ca $^{2+}$ exchangers does not necessarily follow since, in the Na $^+$ /K $^+$ Pump, the regulatory effect of ATP is to accelerate the release of K $^+$ ions from the occluded (E $_2$ K $_2$) conformation after K $^+$ -promoted dephosphorylation.

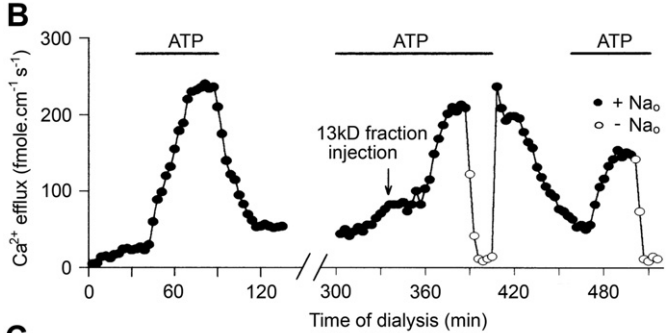
Summarizing, there is no single kinetic scheme that can account for the *trans* effects of the Ca₁²⁺-regulatory site on the extracellular transport sites of the squid nerve or the mammalian heart Na⁺/Ca²⁺ exchanger. In other words, all present models are incomplete. One possible explanation may come from a transport cycle that is more complex than that presently assumed. Cycles consisting of several steps have already been suggested for the heart (Matsuoka and Hilgemann, 1992; Fujioka et al., 2000; Haase et al., 2007; Haase and Hartung, 2009); nonetheless, to account for the data, these extra steps must be influenced by the metabolic regulation of the exchanger. We have not attempted to simulate those complicated models. On the other hand, the explanation may not be related to changes in unidirectional rate constants but rather to modifications in the real affinities of the external transport sites for Na⁺ and Ca²⁺ induced by the state of saturation of the Ca₁²⁺-regulatory sites. Recent studies, by using NMR spectroscopy, indicate that the CBD1 and CBD2 domains of NCX go through an ample range of relative arrangements. In particular, the binding of Ca²⁺ to CBD1 imposes a significant restriction to the inter-domain flexibility (Salinas et al., 2011). This molecular mechanism proposed for the role of CBD1 and CBD2 in NCX function may very well include additional longrange consequences, like changes in the true affinity of the external transport sites.

3. Recent data on metabolic regulation

3.1. The first evidences

Initial experiments in dialyzed squid axon dialysis suggested that ATP stimulation of the squid nerve Na⁺/Ca²⁺ exchanger is a consequence of phosphorylation-dephosphorylation processes. The observations leading to this conclusion (see DiPolo and Beaugé, 1991) were: (a) Mg²⁺ is required but, although it stimulates at low concentration, it becomes inhibitory at concentrations above 1 mM; (b) only hydrolyzable ATP analogs can mimic ATP; ATP-gamma-S, a kinase but not an ATPase substrate, is an even better activator than ATP; (c) pNPP, a phosphatase substrate, and Pi, a phosphatase inhibitor, stimulated MgATP up-regulation; (d) vanadate exhibits a dual action, as activator with a K_i around 5 μ M and as inhibitor with a Ki about 5 mM; this coincides with the Ki's values for phosphatase and kinase inhibition respectively; (e) Cr(III)ATP, a powerful kinase inhibitor, prevents MgATP up-regulation. An additional key observation was that a cytosolic soluble protein of about 13 kDa is essential for MgATP up-regulation, and that this factor becomes phosphorylated in the process. This explained why that up-regulation was not observed in isolated nerve membrane vesicles that lacked cytosolic components and was further supported by the loss of that up-regulation in axons submitted to prolonged dialysis with an 18 kDa cut off capillary. This protein was originally named Soluble Cytosolic Regulatory Protein (SCRP). Fig. 8A illustrates its partial purification by passing the cytosol through filters of decreasing molecular weight cut off and measuring the activity of the filtrate; as can be seen, it disappears in the filtrate of 10 kDa (Beaugé et al., 1996; DiPolo et al., 1997). The 30 kDa filtrated was then passed through a Superdex column and the eluents tested for activity. In isolated vesicles only the fraction around 13 kDa was active. Fig. 8B shows that in a giant axon the MgATP stimulation of Na⁺/Ca²⁺ exchange fluxes is lost after prolonged dialysis, and restored by microinjection of the 13 kDa fraction. On the other hand, other fractions such as the 22 kDa are ineffective (Fig. 8C). Further characterization of SCRP





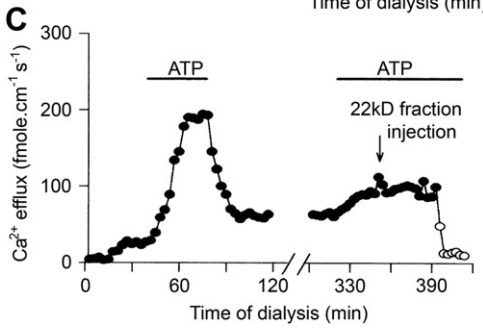


Fig. 8. Initial purification and assay of the cytosolic regulatory protein (SCRP) required for MgATP stimulation of the squid nerve Na⁺/Ca²⁺ exchanger. (A) Partial purification of the SCRP from squid optic ganglia. The bar graph shows the Mean \pm SEM of triplicate experiments on Na $^+$ -gradient-dependent 45 Ca $^{2+}$ uptake in membrane vesicles of squid optic nerves incubated in the presence of 1 mM MgATP. The incubation media also had the filtrates of homogenized optic ganglia passed through filters of different molecular weight cutoff (100, 50, 30 and 10 kDa). The ⁴⁵Ca²⁺ uptake (filled columns) is expressed as a percentage, taking as 100% that observed in the presence of the 12 000 \times g supernatant (0.668 \pm 0.04 nmol mg⁻¹ 10 s⁻¹); the protein content (white columns) is given as a percentage of that seen in the 12 000 x g supernatant $(23.5 \pm 3.8 \text{ mg/ml})$. Notice that a similar value of the fluxes is maintained down to the 30 kDa filtrate; the uptake seen in the 10 kDa filtrate is not different from that observed without MgATP (not shown). (B) Reconstitution of the MgATP stimulation of Na⁺/Ca²⁺ exchange by microiniection of the 13 kD cytosolic protein fraction in a de-regulated dialyzed squid axon. After an initial MgATP stimulation of a Na₀dependent Ca²⁺ efflux, the axons were dialyzed for four hours without ATP and the effect of the nucleotide assayed again before and after the addition of 13 kDa effluent from a Superdex column. Filled symbols correspond to NaSW and open symbols to Na+-free LiSW. Note that the lost MgATP up-regulation is recovered after addition of the 13 kDa fraction. (C) Lack of MgATP stimulation by another protein fraction (22 kDa) microinjection. The experimental conditions are the same as those described in (B) except that the chromatographic fraction used was 22 kDa. Taken from DiPolo et al. (1997) with permission.

showed that: (a) no phosphorylation from Mg[³²P]-γ-ATP was detected in the 30 kDa cytosolic fraction, indicating a lack of autokinase activity; (b) conversely, several bands, including one around 13 kDa, incorporated [³²P]Pi when squid nerve membrane vesicles

were added; i.e. the responsible kinase/s is/are located in the plasma membrane. (c) Staurosporin, at 50–100 μ M, inhibited phosphorylation of most bands in the 30 kDa fraction, but it did not prevent [32 P]Pi incorporation into the 13 kDa; also Staurosporin had no effect on MgATP stimulation of the exchanger; (d) heat denaturation of either the cytosolic fraction or the nerve vesicles prevented both phosphorylation and stimulation of the exchanger; (e) the phosphorylated 30 kDa fraction was able to stimulate Na $^+$ /Ca $^{2+}$ exchange in nerve vesicles even in the absence of ATP. Interestingly however, the simultaneous presence of Mg $^{2+}$ was required (Berberián et al., 2007).

3.2. Identification of SCRP

Peptide sequences obtained by mass spectroscopy of the 13 kDa protein band isolated from the 30-10 kDa cytosolic fraction of squid optic ganglia were matched against a squid expressed sequence tag (EST) database containing approximately 23 000 nucleotide sequences (for ref. see Berberián et al., 2009a). Four peptides matched the predicted amino acid sequence encoded by a single EST sequence with 100% identity (Fig. 9A and B). This EST contains a 405 nucleotide full-length open reading frame and a putative 396 coding sequence that encodes 132 amino acids (Fig. 9C). By BLAST search of NCBI databases it was found that this amino acid sequence matches members of the lipocalin superfamily of lipid binding proteins. The theoretical molecular weight is 14.8 kDa (Berberián et al., 2009a) which agrees with that of the SCRP. The theoretical pI of 5.85 coincides with the acidic nature previously described for SCRP (Berberián et al., 2007). We decided to name it Regulatory Protein of the Squid Na⁺/Ca²⁺ exchanger (ReP1-NCXSQ). The GenBank accession number is EU981897. The number 1 implies the possibility of redundancy (other proteins may have a similar function). NCXSQ generalizes for more than one squid nerve exchanger, because it was found that it acts at least in Loligo pealei, Doritheutis plei, Loligo opalescens and Helix argentinus (Berberián et al., 2009a). In addition, Fig. 9C shows the amino acid sequence used as an antigen to obtain a polyclonal antibody against ReP1-NCXSO. Fig. 9D illustrates the protein patterns from the 30-10 kDa cytosolic fraction from squid optic ganglia samples (Lane 1) and nerve membrane vesicles (Lane 2) run on SDS-PAGE and stained with Coomassie blue. The immunoblot experiments, depicted in the right side of Fig. 9D, shows that a protein band of about 13 kDa of the 30-10 kDa cytosolic fraction (SCRP) reacts with a specific antibody against ReP1-NCXSQ. Another important observation is that the same antibody failed to detect any protein in squid nerve membrane vesicles. These results strongly suggest that ReP1-NCXSQ is identical to the cytosolic component that promotes the MgATP stimulation of squid nerve Na⁺/Ca²⁺ exchanger. Finally, it must be pointed out that the antibody against the recombinant protein was based on the amino acid sequence obtained from the squid gene database. The fact that it detects a native protein in the cytosol of the squid nerve is further evidence that the gene and the protein are one and the same.

3.3. Functional and biochemical characterization of the recombinant ReP1-NCXSQ

ReP1-NCXSQ was expressed in BL21 Escherichia coli and purified; the average yield was 4 mg/L of original culture at a purity of 95% or higher. As expected, the single 13 kDa purified band was recognized by the polyclonal peptide antibody against

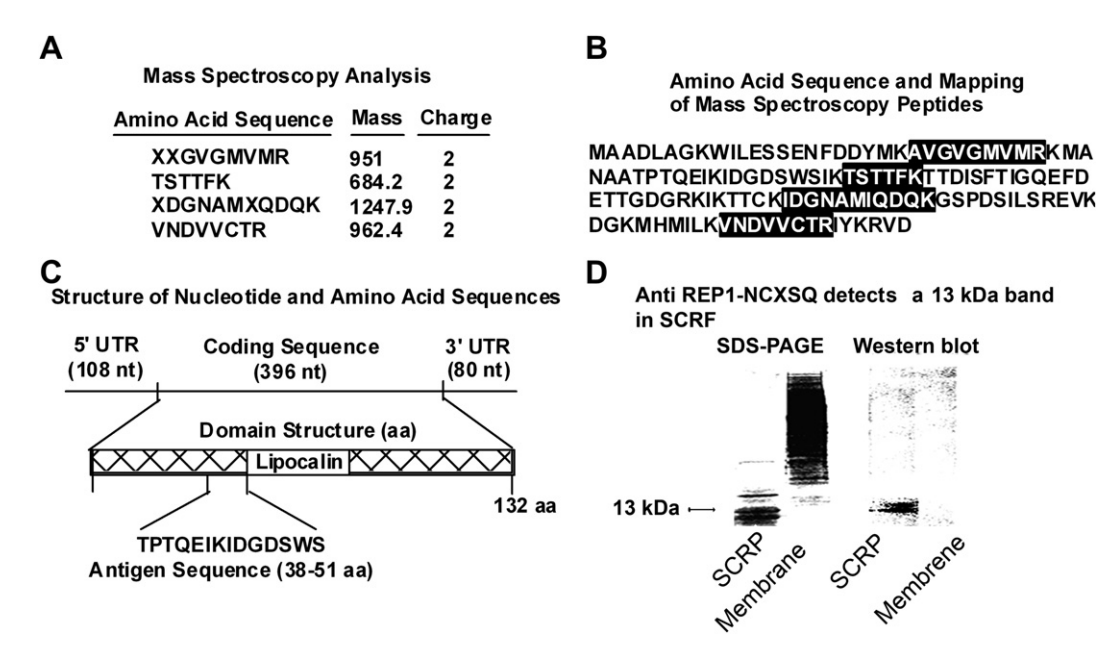


Fig. 9. Identification of the soluble cytosolic protein required for MgATP up-regulation of the squid nerve Na⁺/Ca²⁺ exchanger (ReP1-NCXSQ). (A) Peptides obtained by mass spectroscopy of the 13 kDa cytosolic band phosphorylated during MgATP stimulation of the exchanger. Each of the four peptides has one hundred percent similarity with a lipid binding protein. The figure lists the amino acid sequence, mass and number of charged amino acids. (B) The fourth mass spectroscopy peptides match the full-length amino acid sequence of ReP1-NCXSQ. This mass spectroscopy peptide covers 26% of the RFN amino acid sequence. (C) Schematic representation of the ReP1-NCXSQ nucleotide and amino acid sequence. The tag nucleotide sequence that encodes the protein which matches the peptides obtained by mass spectroscopy contains a 396 nucleotide open reading frame which encodes a 132 amino acid sequence corresponding to a lipid binding protein of the lipocalin super family. The EST also contains elements of the 5′ and 3′ un-translated regions. The amino acid sequence used as an antigen to generate a polyclonal peptide antibody against ReP1-NCXSQ is also shown in the figure. (D) The anti ReP1-NCXSQ detects a 13 kDa band in the 30 kDa cytosolic fraction. Left: Coomassie blue-stained SDS-PAGE (4–20% gradient gel, Invitrogene, USA) of the 30 kDa cytosolic fraction and nerve membranes. Right: Immunoblots. The immunoblots were decorated with a rabbit polyclonal antibody against ReP1-NCXSQ (clone 76g04; Gen Scrip Corp. USA) and then with secondary antibody antirabbit IgC(H + L) alkaline phosphatase conjugate (Pormega, USA) and visualized by phosphorescence (ECF, Amersham-GE, USA) with an image analyzer (Storm 840). On the left, an eight-figure "SCRP" refers to the 30–10 kDa cytosolic fraction from squid optic ganglia (14 μg) and "Membrane" refers to squid nerve membrane vesicles (40 μg). Taken from Berberifan et al. (2009a) with permission.

ReP1-NCXSQ. The ability of ReP1-NCXSQ to promote MgATP upregulation of a Na⁺-gradient dependent Ca²⁺ uptake in squid nerve vesicles was investigated in parallel with a native cytosolic fraction containing SCRP. The assays were conducted in the presence of non-saturating, 1 μM extravesicular Ca²⁺ concentration. Fig. 10 shows that MgATP stimulation of the exchanger is the same with ReP1-NCXSO and the SCRP. In addition, the figure shows that in both cases the stimulation is not affected by 50 uM Staurosporin. a result already seen in dialyzed axons (DiPolo and Beaugé, 2006) and isolated nerve membrane vesicles (Berberián et al., 2009a). Up-regulation of the Na⁺/Ca²⁺ exchanger by MgATP coincides with the phosphorylation of SCRP (Berberián et al., 2009a). Actually, that enabled a band to be spotted around 13 kDa that was subjected to amino acid sequencing. Therefore, if ReP1-NCXSQ is indeed the recombinant SCRP, it must also become phosphorylated under MgATP regulation of the exchanger. This was confirmed in parallel experiments in which either the 30 kDa cytosolic fraction or ReP1-NCXSQ were incubated for 10 s in the low Na⁺ medium used to measure Ca^{2+} fluxes containing 0.5 mM [32 P]- γ -ATP and nerve membrane vesicles as the kinase source. Fig. 10 illustrates typical results where the [32P]Pi incorporation in both preparations is similar in amount and in its insensitivity to Staurosporin. Furthermore, both phosphoproteins remain stable after the centrifugation step carried out to separate them from the membrane vesicles. In addition, as happens with the SCRP (Berberián et al., 2009a), the phosphorylated recombinant ReP1-NCXSQ is able, without the need of ATP, to stimulate the Na⁺-gradient dependent Ca²⁺ uptake in isolated squid nerve vesicles.

3.4. Metabolic regulation in the squid nerve Na⁺/Ca²⁺ exchanger expressed in alien systems

The most extensive studies of the Na⁺/Ca²⁺ exchanger have been carried out in cardiac membrane (patch-clamp and membrane vesicles) and squid nerve (injected, dialyzed axons, and membrane vesicles). Fig. 11A shows the amino acid identity between squid nerve and the canine heart Na⁺/Ca²⁺ exchangers. As a whole, NCXSQ1 is 58% identical to the cardiac exchanger and possesses overall identity (41-64%) with other exchangers. The regions that have functional importance such as the Ca₁²⁺ regulatory binding domain (46% homology), Na_i⁺ inactivation (56% homology), and COOH terminal (70% homology) are well conserved. Furthermore, the α -1 and α -2 repeats involved in ion translocation are well conserved in the two preparations (see Fig. 11A and He et al., 1998). Some basic properties, like stoichiometry of the exchanging cations and regulation by Ca₁²⁺, Na₁⁺, H₁⁺, and ATP, are present in both systems; nevertheless, the presence of fundamental differences between them may provide insight into their structure—function relationships and will certainly facilitate the development of models of the regulatory processes that control the activity of the Na⁺/Ca²⁺ counter-transport. There are, however, substantial functional differences mostly related to regulation. In terms of ionic regulation in the heart, the Na⁺ translocation branch has a marked voltage dependence while in the squid the Na⁺/Na⁺ exchange is voltage insensitive.

But the main differences are seen in the regulation by metabolism. In mammalian heart and nerve, phosphoinositides, and

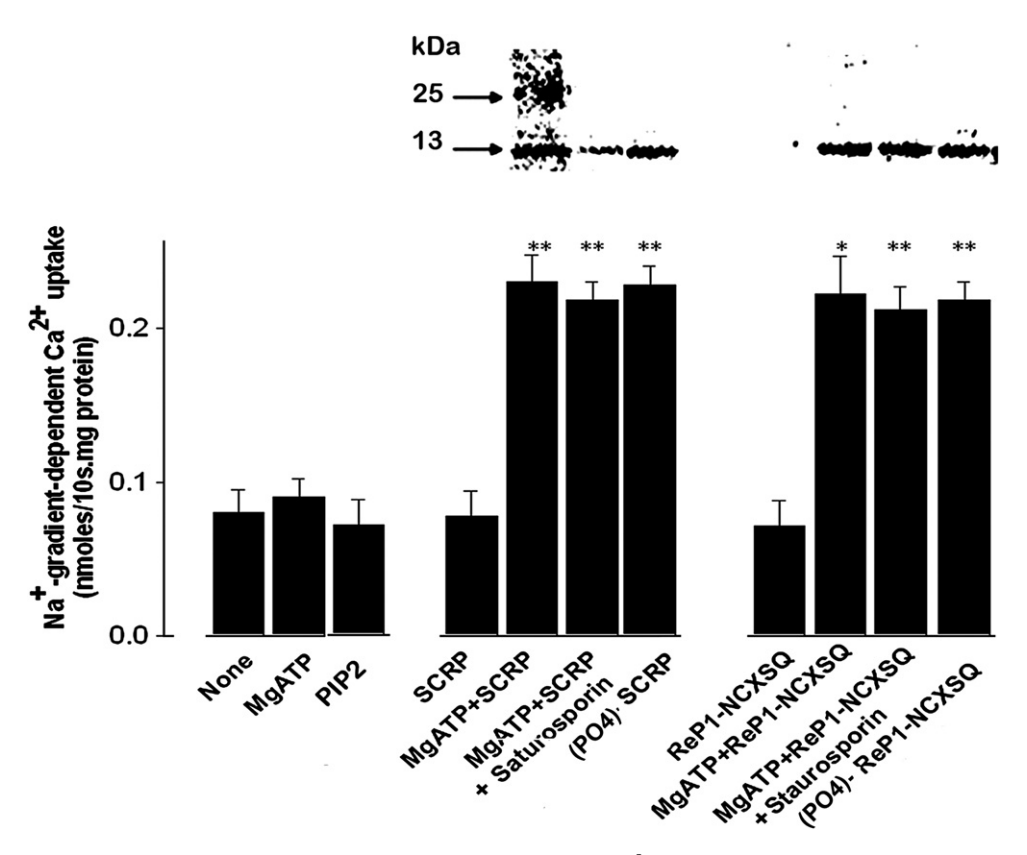


Fig. 10. Comparison between the effects of SCRP and ReP1-NCXSQ on the Na⁺-gradient-dependent Ca²⁺ uptake in squid nerve membrane vesicles and their phosphorylation patterns by Mg[32 P]- γ -ATP. Vesicles were prepared, and the Na⁺-gradient Ca²⁺ uptake estimated as indicated in (DiPolo et al., 1997). The bars represent the Mean \pm SE of triplicate determinations. * $p \le 0.01$ (Student "t" test). Notice: (a) SCRP and ReP1-NCXSQ refer to unphosphorylated, while (PO4)-SCRP and (PO4)-ReP1-NCXSQ refer to previously phosphorylated proteins, i.e., before testing for their effects on Ca²⁺ uptake, SCRP and ReP1-NCXSQ were incubated for 10 s with squid nerve vesicles as a kinase source in the absence and presence of 0.5 mM MgATP. Note that neither the MgATP-stimulated Na⁺-gradient-dependent Ca²⁺ uptake nor the phosphorylation of the 13 kDa band in the 30–10 kDa cytosolic fraction and ReP1-NCXSQ are affected by Staurosporin. Taken from Berberián et al. (2009a) with permission.

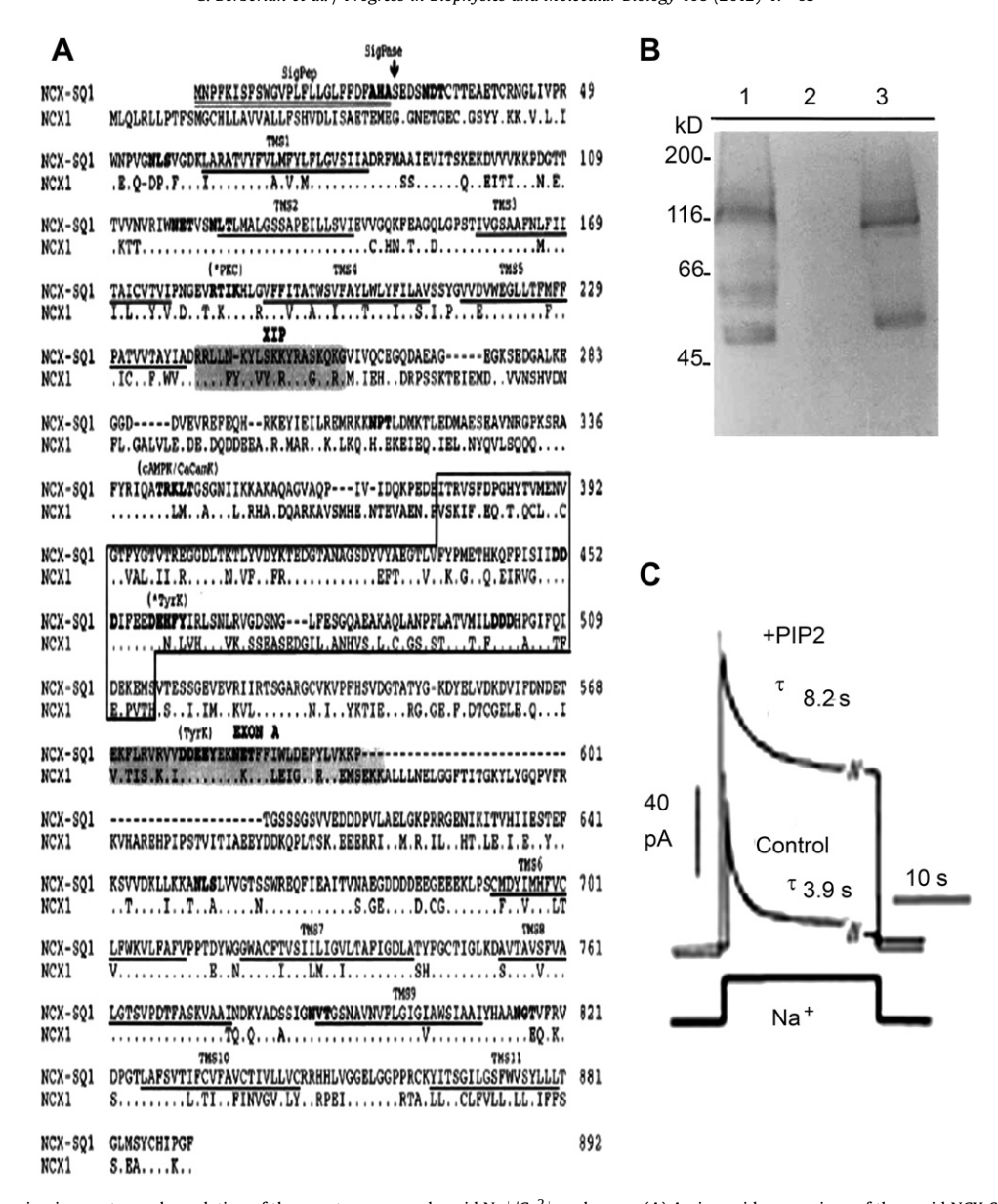


Fig. 11. Sequence, expression in oocytes and regulation of the oocyte-expressed squid Na⁺/Ca²⁺ exchanger. (A) Amino acid comparison of the squid NCX-SQ1 and the canine NCX1 exchanger. (B) Western blot analysis of NCX-SQ1 protein. Protein from squid optical lobe vesicles (lane 1) and oocytes injected with water (lane 2) or cRNA for NCXSQ1 (lane 3) was probed with an antibody raised against a histidine-tagged fusion protein fragment of NCXSQ1. (C) Lack of effect of phosphoarginine (p-ARG) on NCXSQ1 exchange current in an excised oocyte patch. After activation of the exchange current by applying Na1-containing solution, 5 mM phosphoarginine was applied with 3 mM Mg²⁺ (pH 7.0). There is no stimulatory effect, whereas application of 50 μM PtdIns-4,5-P2 (PIP2) strongly stimulates the exchange current to a magnitude more than twice greater than the peak obtained on applying Na⁺ initially. Taken from He et al. (1998), with permission.

particularly PtdIns-4,5-P2 are involved in MgATP stimulation of the Na⁺/Ca²⁺ exchanger (Hilgemann and Ball, 1996; Berberián et al., 1998, 2002); the effect of MgATP takes place through the increase of PtdIns-4,5-P2 in the micro-environment surrounding the antiporter; both NCX1 and PtdIns-4,5-P2 co-immunoprecitate and the amount of PtdIns-4,5-P2 attached to NCX1 is proportional to the stimulation of the exchange fluxes (Berberián et al., 2009b). Conversely, in squid nerve vesicles, MgATP + SCRP activation occurs without any significant change in the patterns of phosphoinositide (PtdIns-4-P and PtdIns-4,5-P2) formation (DiPolo et al., 2004); also, in dialyzed squid axons the injection of PtdIns-PLC at concentrations high enough to reduce the PtdIns levels, or the injection of the PtdIns-4,5-P2 specific antibody have no effect on MgATP modulation of the exchanger (DiPolo et al., 2004). But, and very importantly, although the metabolic pathways for MgATP

modulation are different in both species, they concur in similar changes of the kinetic parameters that influence the ionic interactions with the large intracellular loop.

3.4.1. Expression in frog oocytes

When the recombinant NCXSQ1 expressed in *Xenopus laevis* oocytes was probed with an antibody raised against a histidine-tagged fusion protein fragment of NCXSQ1 it showed a protein pattern similar to that of the NCXSQ protein obtained from squid optical lobe (see Fig. 11B). On the other hand, its metabolic regulation showed discrepancies with that observed in the constitutive exchanger of squid nerve; surprisingly, it displayed a regulation similar to that observed in NCX1 either in cardiomyocytes or when expressed in frog oocytes (He et al., 1998). Thus, MgATP upregulation of frog oocyte-expressed NCXSQ1 was mimicked by

PtdIns-4,5-P2, (Fig. 11C) and abolished by a PtdIns-4,5-P2 antibody (not shown here). In addition, phosphoarginine, which stimulates the squid exchanger in dialyzed axons and membrane vesicles, has no effect on NCXSQ1 expressed in oocytes (He et al., 1998).

3.4.2. Expression in yeast

The unexpected metabolic regulation of frog oocyte-expressed NCXSQ1 may find an explanation in the different biochemical composition of the squid nerve and oocyte membranes, and/or the kinases attached to them. Any rate, it is obvious that it represents a serious obstacle for an attempt to use that preparation for further analyzing biochemical aspects of that regulation. For that reason we looked for another system, using *Saccharomyces cerevisiae*

(Raimunda et al., 2009). In these experiments the exchanger was fused to the enhanced green fluorescence protein (eGFP) on its C-terminus and had two tags, a Strep-tag II and 6 histidines, added to the N-terminal region (ST-6HB-NCXSQ1-eGFP). The eGFP fluorescence signal co-localized with that of the plasma membrane marker FM1-43 in whole cells that displayed an uptake of Ca $^{2+}$ with the expected characteristics of the reverse Na $^+$ /Ca $^{2+}$ exchange mode (see Raimunda et al., 2009 and Fig. 12A). Similar to squid nerve membrane vesicles, inside-out yeast plasma membrane vesicles (ISOV) showed a Ca $^{2+}$ regulation of the forward mode (see Fig. 12B). As these figures show, the apparent $K_{\rm ms}$ for extravesicular Ca $^{2+}$ displayed close values, i.e., $4.93~\pm~0.76~\mu{\rm M}$ for the squid nerve membrane vesicles and $4.53\pm0.83~\mu{\rm M}$ for the inside-out yeast plasma membrane vesicles. In

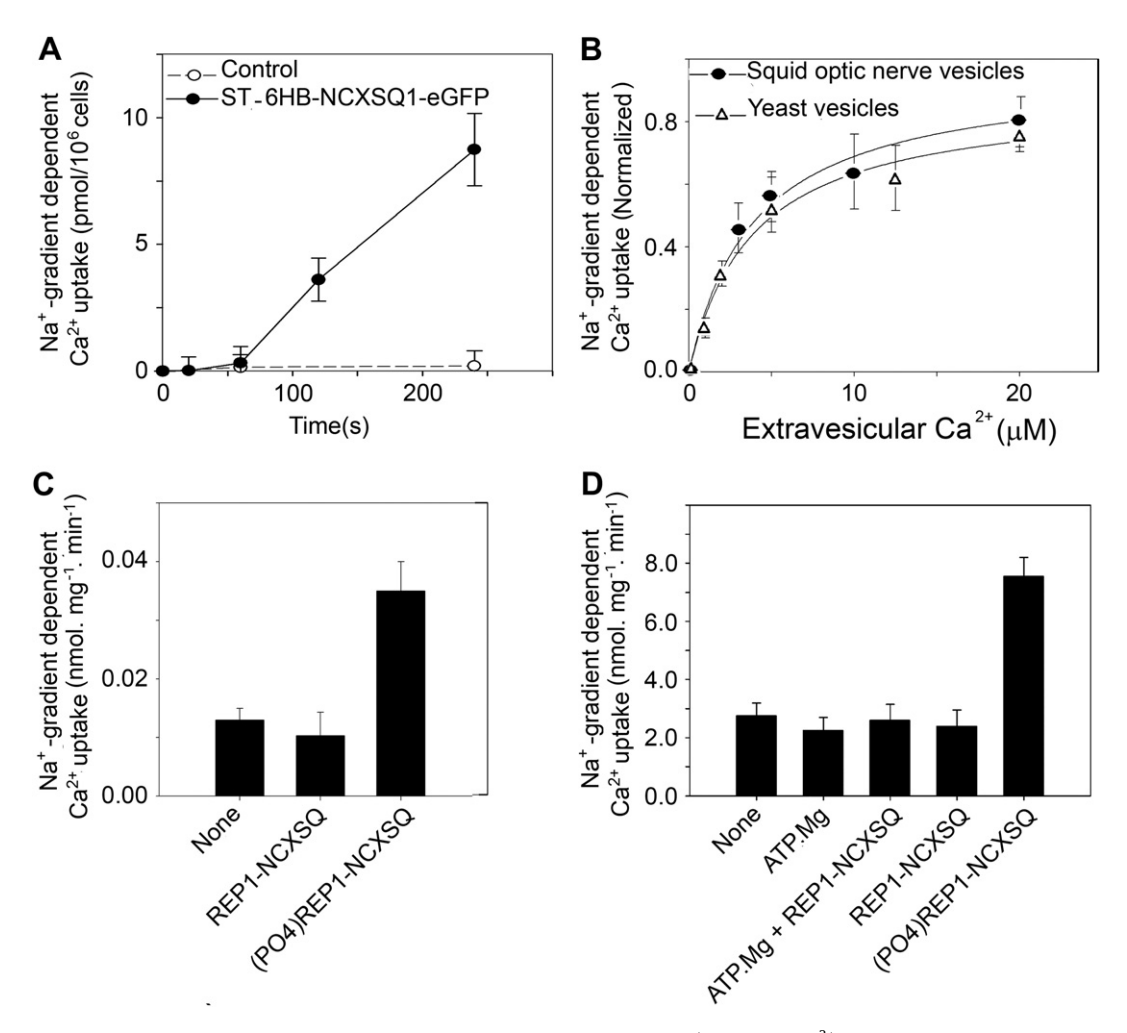


Fig. 12. Functional expression and metabolic regulation of NCXSQ1 in yeast. (A) Time dependence of Na⁺-dependent Ca²⁺ uptake in whole yeast cells by "reverse mode" of the Na⁺/Ca²⁺ exchange in S. cerevisiae transformed with pKS1-ST-6HB-NCXSQ1-eGFP or pKS1-ST (Controls). To clamp intra- and extracellular monovalent cation concentration, cells were pre-incubated 4 min in 140 mM NaCl or KCl with 20 μg/ml gramicidin (pH 7.4 at 20 °C with 20 mM Mops-Tris). The uptake reaction was started by addition of 200 μM ⁴⁵Ca²⁻¹ (50.000 c.p.m./nmol) to these media (see Raimunda et al., 2009, and Urbanczyk et al., 2006). Values represent mean \pm S.E. (n=4). Note that cells expressing exchanger construct, but not cells with the empty vector (Control), showed Na⁺/Ca²⁺ exchange activity. (B) Comparison of extravesicular Ca²⁺ concentration (cytosolic [Ca²⁺]) dependence between the Na⁺-gradient dependent Ca²⁺ uptake in inside-out yeast plasma membrane vesicles from yeast cells transformed with pKS1-ST-6HB-NCXSQ1-eGFP and squid nerve vesicles. Influxes of 45Ca²⁺ were measured during 10 s by incubating the vesicles at 20 °C in solutions with 150 mM NaCl or 7.5 mM NaCl + 142.5 mM KCl, 70 mM sucrose, 1 mM free Mg²⁺, 10 mM Mops-Tris (pH 7.4 at 20 °C), 0.150 mM EGTA, 0.2 mM vanadate, and the indicated free [Ca²⁺]. In the case of yeast vesicles, all values are the difference between total uptake and that obtained in vesicles of cells transformed with empty vector. The data points represent the mean \pm S.E. (n = 3). The lines through the points are the best fit to a Michaelian equation with a Km of $4.53 \pm 0.83 \,\mu\text{M}$ and $4.93 \pm 0.76 \,\mu\text{M}$ to yeast plasma membrane vesicles and squid nerve vesicles respectively. (C) Previously phosphorylated ReP1-NCXSQ up-regulates Na⁺/Ca²⁺ exchange activity of inside-out plasma membrane vesicles of yeast expressing ST-6HB-NCXSQ1 in the absence of ATP. Na⁺/Ca²⁺ exchange was measured as indicated in (B), in the absence of ATP without ReP1-NCXSQ and with unphosphorylated (ReP1-NCXSQ) or previously phosphorylated ReP1-NCXSQ ((PO4)ReP1-NCXSQ). The Ca^{2+} concentration was 3 μM in all cases. Each bar represents the mean ± S.E. (n = 4). (D) (PO4)ReP1-NCXSQ up-regulation of Na⁺-gradient-dependent Ca²⁺ uptake in proteoliposomes containing purified ST-6HB-NCXSQ1-eGFP. The proteoliposomes were equilibrated with solutions containing 150 mM NaCl and 20 mM Mops-Tris, pH 7.0 at 20 °C. Influxes of 45Ca²⁺ were measured during 60 s at 20 °C as indicated above. Values are mean \pm S.E. (n = 4). Note that the exchange activity is up-regulated only in the presence of 0.5 µg phosphorylated ReP1-NCXSQ ((PO4)ReP1-NCXSQ; 0.36 μM) while it is not affected by the same amount of unphosphorylated ReP1-NCXSQ1 nor by 1 mM MgATP in the absence of ReP1-NCXSQ1 (unpublished data from DiPolo, Berberián and Beaugé and redrawn, with permission from Raimunda et al., 2009).

addition, Fig. 12C illustrates an important result, indicating that insideout yeast plasma membrane vesicles that expressed ST-6HB-NCXSQ1-eGFP protein were modulated by previously phosphorylated ReP1-NCXSQ, as was observed in squid nerve membrane vesicles (Berberián et al., 2009a). Another additional crucial observation was that, in proteoliposomes containing only the ST-6HB-NCXSQ1-eGFP protein, Na⁺/Ca²⁺ exchange was stimulated by phosphorylated ReP1-NCXSQ; i.e., this up-regulation needs no other requirement except the lipid membrane and the exchanger protein (see Fig. 12D). Therefore, the exchanger expressed in yeast retains the MgATP regulation observed in dialyzed squid axons and in isolated membrane vesicles from squid nerve.

3.5. Possible pathways involved in the ReP1-NCXSQ dependent metabolic regulation of squid Na^+/Ca^{2+} exchanger

As happens with the PtdIns-4,5-P2 mediated MgATP regulation of NCX1, we still do not know the intimate mechanism by which ReP1-NCXSQ-mediated MgATP modulation of NCXSQ takes place. An

interaction of the phosphorylated cytosolic factor (PO4-ReP1-NCXSQ) may be direct or indirect through other structure/s. The C-terminal part of the regulatory loop may provide an option for a direct interaction. This region is strongly hydrophobic and has the highest similarity (75%) between NCX1 and NCXSQ1 (He et al., 1998); that environment could provide an anchorage region for ReP1-NCXSQ; actually, the need for phosphorylation may be explained if that process leads to the proper conformation required for binding. This idea finds some support in the fact that lipocalins can attach to macromolecules (Arnold et al., 2005).

Another mechanism could be the simultaneous requirement of another structure; i.e. the exchanger protein is not the target for phosphorylated ReP1-NCXSQ. This would offer several possibilities: (a) transphosphorylation, in which PO4-ReP1-NCXSQ transfers its phosphate to another molecule that eventually interacts with the exchanger. A mechanism of this kind is found in the immunoglobulin E receptor signaling that concurs with a lipid—protein interaction (Holowka et al., 2007). (b) A removal by PO4-ReP1-NCXSQ of a membrane lipid having an inhibitory effect of the exchanger, as has

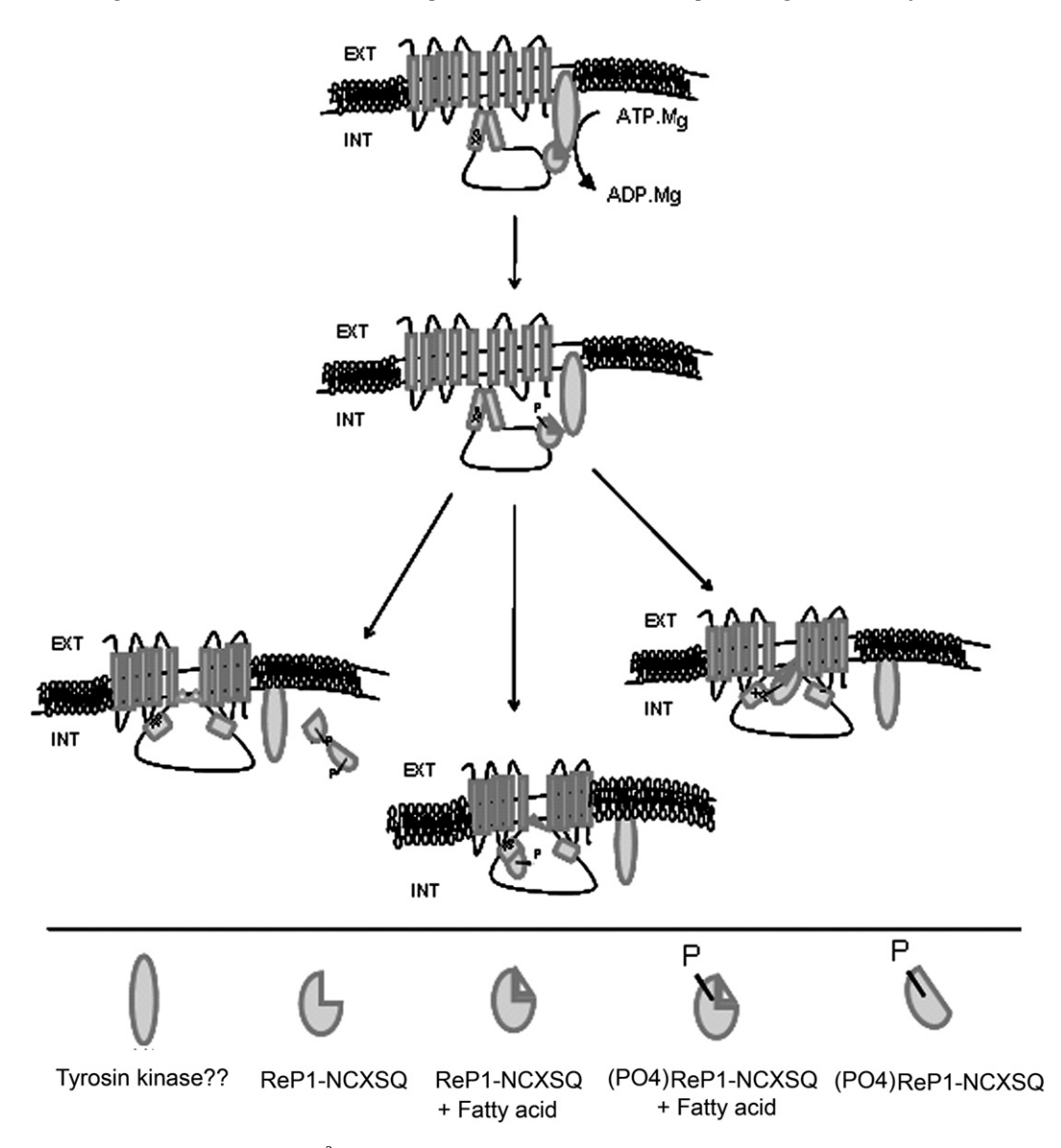


Fig. 13. Cartoon illustrating possible mechanisms of Na⁺/Ca²⁺ exchanger regulation by MgATP and REP1-NCXSQ. Out means extracellular side; in represents intracellular side. Notice: (i) the XIP (exchange inhibitory peptide) region is on the cytoplasmic regulatory loop; (ii) + means a basic region; (iii) – refers to an acidic region. (Taken, with permission, from Fig. 4.1 of D. Raimunda's doctoral study: "Expresión y purificación de la proteína NCXSQ1 de calamar en *Saccharomyces cerevisiae*: aplicación a estudios de regulación metabólica del transporte Na⁺/Ca²⁺ⁿ, Universidad Nacional de Córdoba, Argentina, April 2009).

been proposed for LBP activation of the Na⁺-dependent amino acid uptake in brain synaptosomes (Bass et al., 1984). (c) Opposite to (b), by promoting the interaction of an activator lipid with the transporter. Regarding the last two possibilities, we found that ReP1-NCXSQ binds polyphosphoinositides and phosphatides but does not seem to interact with Cholesterol, Sphingomyelin, Phosphoserine, Phosphoetanolamide or PtdIns (Berberián et al., 2009a).

One could also consider the interaction of ReP1-NCXSQ with lipids. In fact, when expressed in *E. coli*, this protein elutes from the Ni²⁺-NTA affinity column together with an intra barrel fatty acid. Perhaps the presence of that lipid is what promotes its activity, as occurs with FABP from several sources (Buelt et al., 1991, 1992). Even more, it is possible to conceive that the single entrance-exit door or mouth for the fatty acid (see Crystal structure) is sensitive to the state of phosphorylation. The fact that vanadate increased the magnitude of MgATP stimulation of the squid nerve Na⁺/Ca²⁺ exchanger may just mean that the role of vanadate is to prolong the half-life of phosphorylated species, thereby increasing the probability of interaction with its target. A cartoon illustrating this type of mechanism is pictured in Fig. 13.

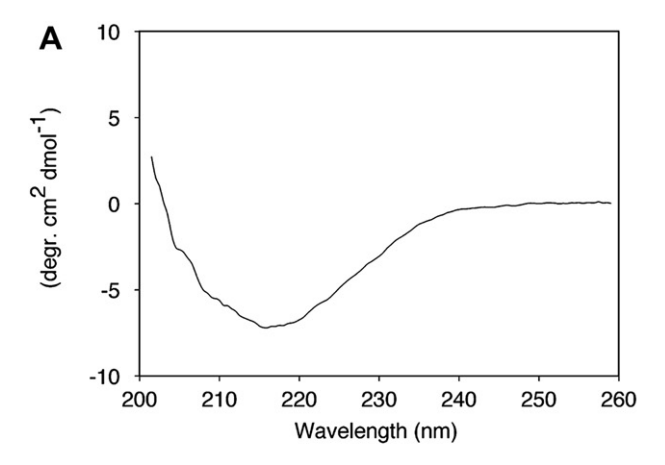
4. Structure of ReP1-NCXSQ

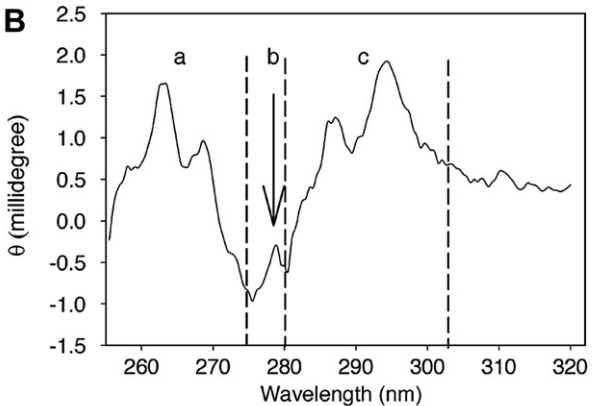
4.1. Spectral analysis

Fig. 14A illustrated one of the Far-UV CD spectra of ReP1-NCXSQ showing a broad negative band centered at 215 nm typical of proteins containing a sizable number of β -strands in the secondary structure (Venyaminov and Yang, 1996). These structures are also expected to display a positive band at 195 nm. However, in our case this would be masked by the strong absorption of the buffer used in these assays (not shown).

The Near-UV CD spectrum of Fig. 14B has three well-defined groups of bands characteristics of local anisotropy environment corresponding to the local environment of the lateral chains of amino acids in folded proteins with a defined tertiary structure, (Woody and Dunker, 1996). This spectral shape is remarkably similar to that observed for the intestinal fatty-acid binding protein (IFABP) (Clérico and Ermácora, 2001). The sharp bands between 250 and 275 nm are likely to correspond to the absorption of Phe residues, the peak at 279 to Tyr residues and the double peak above 280 nm to Trp residues. This kind of spectrum with highly-structured bands agrees with the existence of a protein with a well-defined tertiary structure in its the native state.

Fig. 14C depicts an infrared absorbance spectrum. Between 1600 and 1700 cm⁻¹ there is an amide I' band attributed primarily to the C=O stretching of the peptide bonds providing information on the secondary structure of ReP1-NCXSQ (Byler and Susi, 1986). Similar results, obtained with fatty acidbinding proteins from human liver and heart (Tanfani et al., 1995), adipocytes (Gericke et al., 1997) and avian liver (Nolan et al., 2003) agree quite well with a protein containing a majority of β -strands in its structure. The Fourier self deconvolution in the upper trace in Fig. 14C, and the second derivative (not shown), allows the components to be identified (Kauppinen et al., 1981). Thus, the fitting of the original (not deconvoluted) spectrum assuming a Gaussian shape (see Arrondo and Goñi, 1999) gives six components; particularly important if the band at $1626\ cm^{-1}$ also observed in the avian liver PABP and in several other proteins like concanavalin A, lipophilin, apo B-100 and a lentil lectin (Nolan et al., 2003). In addition, the bands centered at 1639 and 1672 cm⁻¹ can be assigned to β -sheet chains and that at 1651 cm⁻¹ is due to α -helical structures while those at 1662 and $1684\,\mathrm{cm^{-1}}$ to turns and bends (Byler and Susi, 1986). The area under the component bands can be accurately considered





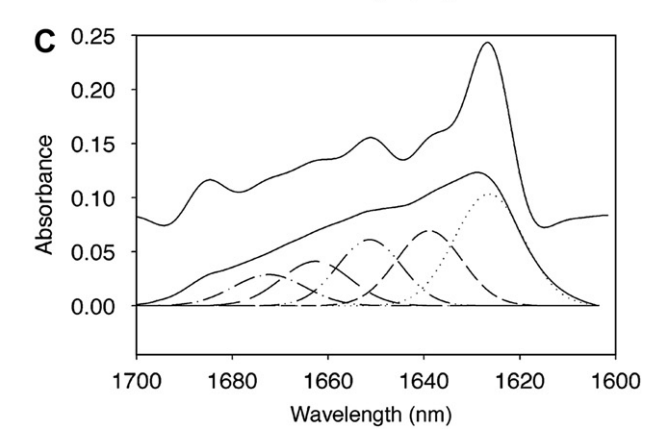


Fig. 14. Circular dichroism and Amide I' infrared absorption spectrum analysis of ReP1-NCXSQ. (A) Far-UV Circular dichroism: The ordinate is the ellipticity calculated by mean residue molecular weight. The solution contained 10 μ M ReP1-NCXSQ in 50 mM Tris-HCl (pH RT 7.3), 30 mM NaCl and 100 mM NMG-Cl. (B) Near-UV Circular dichroism: The ordinate is the measured ellipticity. The sample contained 69 μM ReP1-NCXSQ in 50 mM Tris-HCl (pH RT 7.3), 30 mM NaCl and 100 mM NMG-Cl. Note: (a) bands between 250 and 275 nm that can be assigned to the absorption of Phe residues; (b) the peak at 279 (c) associated to Tyr residues; (c) double peak above to 280 due to the absorption of Trp residues. The appearance of these highly structured bands is indicative that the protein is in the native state with a well-defined tertiary structure. (C) Amide I' infrared absorption spectrum: The middle trace is the experimental spectrum. Upper trace is the Fourier self-deconvoluted spectrum using a bandwidth of 18 cm⁻¹ and a narrowing factor k = 2. The Gaussian curves under the experimental spectrum are the band components obtained by Fourier self deconvolution and band fitting. The absorbance scale corresponds to the experimental spectrum. (Taken from Berberián et al., 2009a with permission).

proportional to the amount of the corresponding secondary structures. On those basis, the total area to β -structures (1626, 1639 and 1672 cm⁻¹) sums 63% of the amide I' area, while the α -helix band corresponds to 18% of the total area. Taking

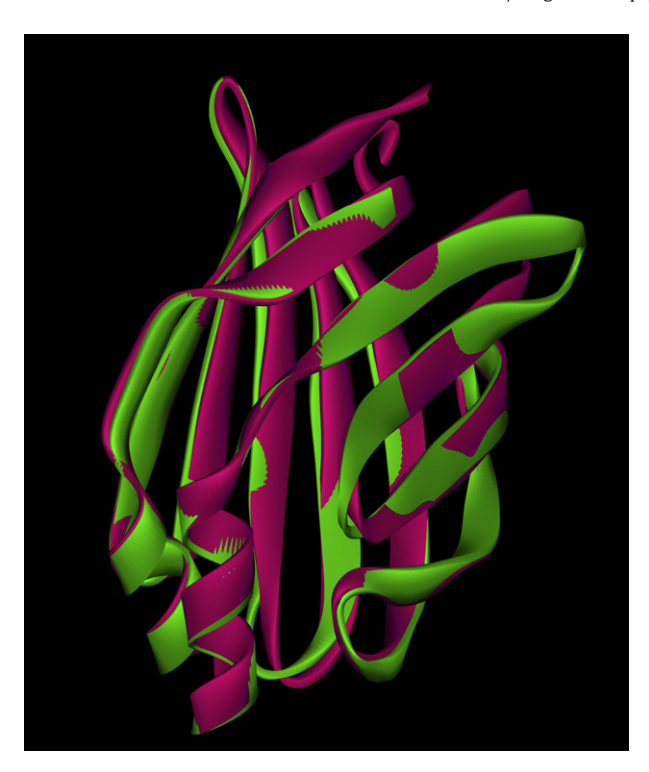


Fig. 15. Comparison between the predicted and the solved crystal structure of ReP1-NCXSQ. The Blast ribbon structure predicted from the amino acids sequence is shown in green and the ribbon representation of the crystallographic structure in magenta. Note that the structure folds in a β -sandwich, with 10 β -sheets, typical of lipid-binding proteins.

together, the spectral data coincides with that expected from the structure predicted on the basis of the primary amino acid sequence (see below).

4.2. Predicted and solved crystal structure of ReP1-NCXSQ

A Blast search with the amino acidsof the sequence of ReP1-NCXSQ produced a protein corresponding to the lipid binding families; the highest degree of sequence identity (58%) was with the shrimp cellular retinoic acid/retinol binding protein. Both, the predicted and the recently solved crystal structure of ReP1-NCXSQ (unpublished) are shown over imposed in Fig. 15. The ribbon representation of the structure predicted from the sequence (green ribbon) agrees rather well with that obtained from crystallographic analysis (magenta ribbon). Note that the structure folds in a β -sandwich, with 10 β -sheets, typical of lipid-binding proteins. Additional data not presented here indicates that the carboxylate head of the lipid makes strong contacts with Tyr 128 and Arg 126.

5. Concluding remarks. Comparison with other systems

The requirement of a cytosolic protein for MgATP up-regulation of the squid nerve Na^+/Ca^{2+} exchanger does not seem to be the only case of ion transporter metabolic regulation. Metabolic regulators may involve direct interaction with the transporting molecule, or the effect may be indirect, acting on other structures including membrane components. As particular examples: (1) In the mammalian heart, phospholemman (PLM), the first cloned member of the FXYD family of ion transport regulators, modulates the activities of both Na^+/K^+ -ATPase and the cardiac Na^+/Ca^{2+} exchanger (NCX1). PLM, when phosphorylated at Ser68, disinhibits Na^+/K^+ -ATPase and actively inhibits NCX1 (Song et al., 2008). (2) 14-3-3 proteins are

phosphoserine-binding proteins that modify the activities of a wide array of targets via direct protein—protein interactions. In animal cells, the majority of their known targets are involved in signal transduction and transcription. In plants, we know about them primarily through their regulation of the plasma membrane H⁺-ATPase and carbon and nitrogen metabolism enzymes (Bunney et al., 2002). In relationship with the Na^{+/}Ca²⁺ exchanger (Pulina et al., 2006), the screening of the human brain cDNA library identified the ε - and ς isoforms of the 14-3-3-protein family as interacting partners of the cytosolic loop of the NCX2 exchanger. The interaction was confirmed by immunoprecipitation and in vitro binding experiments. The effect of the interaction on the homeostasis of Ca²⁺ was investigated by co-expressing NCX2 and 14-3-3 in HeLa cells together with the recombinant Ca²⁺ probe aequorin; the ability of cells expressing both NCX2 and 14-3-3 to dispose of a Ca²⁺ transient induced by an InsP3-producing agonist was substantially decreased, indicating a reduction of NCX2 activity. The 14-3-3-protein also inhibited the NCX1 and NCX3 isoforms (Pulina et al., 2006). (3) MgATP-dependent PtdIns-4,5-P2 production, sometimes associated with signal transduction pathways, modulates K⁺ channels and the mammalian heart Na⁺/Ca²⁺ exchanger (NCX1) (Hilgemann, 1997). Actually, in the case of NCX1, a close association of the exchanger with a PtdIns(4)-5 kinase is essential to optimize upregulation (Berberián et al., 2009b; Forcato et al., 2010). In most cases, PtdIns-4,5-P2 increases channel activity (Suh and Hille, 2008); however, in some others its effect is the reverse, as happens in the visual excitation process of microvillar light receptors where, in a direct signaling role, it acts as an inhibitor (Gomez and Nasi, 2005). (4) Acvl CoAs are endogenous activators of NCX1, exhibiting chain length and saturation dependence, the longer chain saturated acvl moieties being the most effective. In addition, Acyl CoAs may interact directly with the XIP (exchanger inhibitory peptide) sequence, a known region of anionic lipid modulation, to dynamically regulate NCX1 activity and Ca²⁺ homeostasis (Riedel et al., 2006). (5) The NCX1 mammalian isoform has a PKC-dependent up-regulation that does not lead to phosphorylation of the exchanger; to account for this result, it was proposed that the signal transmission induced by PKC activators requires a cytosolic molecule (Iwamoto et al., 1998). Furthermore, the need for cytosolic regulatory proteins has also been suggested for MgATP modulation of the NHE1 sodium-proton exchanger (Aharonovitz et al., 1999). (6) The regulation of Na⁺/K⁺-Pump (or Na⁺/K⁺-ATPase) includes substrates, cytoskeletal components, the γ -subunit and like proteins, endogenous inhibitors and hormones such as corticosteroids, peptides and catecholamines (Therien and Blostein, 2000). (7) The plasma membrane Ca²⁺-ATPases, practically still at low Ca²⁺ concentrations, requires calmodulin, acid phospholipids and protein kinases to become active. Also proteins such as MAGUK, NHERF and calcineurin A regulate their function by sorting some of them to specific regions of the cell membrane (Di Leva et al., 2008). (8) Another model of regulators is those generally known as 2-component systems.

Most prokaryotic signal-transduction systems and a few eukaryotic pathways use phosphotransfer schemes involving two conserved components, a histidine protein kinase and a response regulator protein. The histidine protein kinase, which is regulated by environmental stimuli, autophosphorylates at a histidine residue, creating a high-energy phosphoryl group that is subsequently transferred to an aspartate residue in the response regulator protein. Phosphorylation induces a conformational change in the regulatory domain that results in activation of an associated domain that affects the response. Two-component systems are found in organisms of all domains: Eubacteria, Archaea, and Eukarya. However, their abundance in each domain differs substantially. His/Asp phosphotransfer systems account for the majority of signaling pathways in eubacteria but are quite rare in eukaryotes, in which kinase cascades involving Ser/Thr and Tyr

phosphorylation predominate. In eukaryotes, His/Asp phosphorelays are coupled to mitogen-activated protein (MAP) kinase cascades and a cAMP-dependent protein kinase (see Stock et al., 2000). Before ReP1-NCXSQ was identified, this type of system was proposed as a possible mechanism involving the MgATP upregulation of NCXSQ1 (Beaugé et al., 1996). We searched for such a system in the squid with negative results (unpublished experiments). Phosphorylated ReP1-NCXSQ can stimulate squid Na⁺/Ca²⁺ exchange fluxes even in the absence of the nucleotide. Interestingly, as happens with ATP, that stimulation does not take place in the absence of millimolar [Mg²⁺]. This may suggest that a transphosphorylation takes place (from the factor to another structure) or that the binding of this phosphorylated protein to its target is Mg²⁺ dependent.

Finally, one of the most interesting features of the regulation, kinetics and transport of ions through the Na $^+$ /Ca $^{2+}$ exchanger is that ions (Na $^+$, H $^+$ and Ca $^{2+}$) and metabolic substrates regulate the rate of Ca $^+$ and Na $^+$ transport, both inward and outward, by acting only at the intracellular regulatory loop and not at the transport sites. This strongly suggests that in the near future the control of exchange activity by pharmacological means is most likely to be focused on developing drugs that target sites within the intracellular loop.

Acknowledgments

The work was supported by Grants from the US National Science Foundation (MCB 0444598), Fondo Nacional para Investigaciones Científicas y Tecnológicas (PICT-05-38073) and Consejo Nacional de Investigaciones Científicas y Técnicas (PIP 2010-2012: GI11220090100063), Argentina, Fondo Nacional para Ciencia y Técnica (S1-9900009046 and G-2001000637 FONACIT) and Fundación Polar, Venezuela and CNRS, INSERM, Strasbourg, France.

References

- Aharonovitz, O., Demaurex, N., Woodside, M., Grinstein, S., 1999. ATP dependence is not an intrinsic property of Na⁺/H⁺ exchanger NHE1: requirement for an ancillary factor. Am. J. Physiol. 276, C1303–C1311.
- Arnold, K., Bordoli, L., Kopp, J., Schwede, T., 2005. The SWISS-MODEL workspace: a web-based environment for protein structure homology modelling. Bio-informatics 22, 195–201.
- Arrondo, J.L., Goñi, F.M., 1999. Structure and dynamics of membrane proteins as studied by infrared spectroscopy. Prog. Biophys. Mol. Biol. 72, 367–405.
- Baker, P.F., Glitsch, H.G., 1973. Does metabolic energy participate directly in the Na⁺-dependent extrusion of Ca²⁺ ions from squid giant axons? J. Physiol. (London) 233. 44–46.
- Baker, P.F., McNaughton, P.A., 1976. Kinetics and energetic of calcium efflux from intact squid giant axon. J. Physiol. (London) 259, 103–144.
- Bass, N., Raghupathy, R., Rhoads, D.E., Manning, J.A., Ockner, R.R., 1984. Partial purification of molecular weight 12 000 fatty acid binding proteins from brain and their effect on synaptosomal Na⁺-dependent amino acid uptake. Biochemistry 23, 6539–6544.
- Beaugé, L., DiPolo, R., 2008. Dual effect of Na_i⁺ on Ca²⁺ influx through the Na⁺/Ca²⁺ exchanger in dialyzed squid axons. Experimental data confirming the validity of the squid axon kinetic model. Am. I. Physiol. Cell. Physiol. 294. C118—C125.
- the squid axon kinetic model. Am. J. Physiol. Cell. Physiol. 294, C118—C125. Beaugé, L., DiPolo, R., 2009. The squid axon Na⁺/Ca²⁺ exchanger shows ping-pong kinetics only when the Ca_i-regulatory site is saturated. Cell. Physiol. Biochem. 23, 37—42.
- Beaugé, L., Girardi, D., Rojas, H., Berberian, G., Di Polo, R., 1996. A nerve cytosolic factor is required for MgATP stimulation of Na⁺-gradient- dependent Ca⁺ uptake in plasma membrane vesicles from squid optic nerve. Ann. N.Y. Acad. Sci. 779, 208–216.
- Berberián, G., Hidalgo, C., DiPolo, R., Beaugé, L., 1998. ATP stimulation of Na⁺/Ca²⁺ exchange in cardiac sarcolemmal vesicles. Am. J. Physiol. 274, C724–C733.
- Berberián, G., Asteggiano, C., Pham, C., Roberts, G., Beaugé, L., 2002. MgATP and phosphoinositides activate Na/Ca exchange in bovine brain vesicles. Comparison with other Na/Ca exchangers. Pflugers Arch. Eur. J. Physiol. 444, 579–585.
- Berberián, G., DiPolo, R., Beaugé, L., 2007. Some biochemical properties of the upregulation by MgATP and phosphoarginine of the squid nerve Na⁺/Ca²⁺ exchanger. Ann. N.Y.Acad. Sci. 1099, 152–165.

- Berberián, G., Bollo, M., Montich, G., Roberts, G., DeGiorgis, J., DiPolo, R., Beaugé, L., 2009a. A novel lipid binding protein is a factor required for MgATP stimulation of the squid Na/Ca exchanger. Biochim. Biophys. Acta Biomembranes 1788, 1255—1262.
- Berberián, G., Forcato, D., Beaugé, L., 2009b. Key role of a Ptdlns-4,5-P2 micro domain in ionic regulation of the mammalian heart Na⁺/Ca²⁺ exchanger. Cell Calcium 45, 546–553.
- Bers, D., 1999. Excitation-Contraction Coupling and Cardiac Contractile Force, vol. 122. Kluwer Academic Publisher, Norwell, MA.
- Blaustein, M.P., 1977a. Sodium ions, calcium ions, blood pressure regulation, and hypertension: a reassessment and a hypothesis. Am. J. Physiol. 232, C165—C173.
- Blaustein, M.P., 1977b. Effects of internal and external cations and ATP on sodium—calcium exchange and calcium—calcium exchange in squid axons. Biophys. J. 20, 79—111.
- Blaustein, M.P., Lederer, J.N., 1999. Sodium/Calcium exchange: its physiological implication. Physiol. Rev. 79, 763–854.
- Boscia, F., Gala, R., Pannaccione, A., Secondo, A., Scorziello, A., Di Renzo, G., Annunziato, L., 2009. NCX1 expression and functional activity increase in microglia invading the infarct core. Stroke 40, 3608–3617.
- Brinley, F.J., Mullins, L.J., 1967. Sodium extrusion by internally dialyzed squid axons. J. Gen. Physiol. 50, 2203–2231.
- Buelt, M.K., Shekels, L.L., Jarvis, B.W., Bernlohr, D.A., 1991. In vitro phosphorylation of the adipocyte lipid-binding protein (p15) by the insulin receptor. Effects of fatty acid on receptor kinase and substrate phosphorylation. J. Biol. Chem. 266, 12266–12271
- Buelt, M.K., Xu, Z., Banaszak, L.J., Bernlohr, D.A., 1992. Structural and functional characterization of the phosphorylated adipocyte lipid-binding protein (p15). Biochemistry (USA) 31, 3493–3499.
- Bunney, T.D., van den Wijngaard, P.W., Boer, A.H., 2002. 14-3-3 protein regulation of proton pumps and ion channels. Plant Mol. Biol. 50, 1041–1051.
- Byler, D.M., Susi, H., 1986. Examination of the secondary structure of proteins by deconvolved FT-IR spectra. Biopolymers 25, 469–487.
- Clérico, E.M., Ermácora, M.R., 2001. Tryptophan mutants of intestinal fatty acid-binding protein: ultraviolet absorption and circular dichroism studies. Arch. Biochem. Biophys. 395, 215–224.
- Cuomo, O., Gala, R., Pignataro, G., Boscia, F., Secondo, A., Scorziello, A., Pannaccione, A., Viggiano, D., Adornetto, A., Molinaro, P., Li, X.F., Lytton, J., Di Renzo, G., Annunziato, L., 2008. A critical role for the potassium-dependent sodium—calcium exchanger NCKX2 in protection against focal ischemic brain damage. J. Neurosci. 28, 2053—2063.
- Di Leva, F., Domi, T., Fedrizzi, L., Lim, D., Carafoli, E., 2008. The plasma membrane Ca²⁺-ATPase of animal cells: structure, function and regulation. Arch. Biochem. Biophys. 476, 65–74.
- DiPolo, R., 1974. Effect of ATP on the calcium efflux in dialyzed squid giant axons. J. Gen. Physiol. 64, 503–517.
- DiPolo, R., Beaugé, L., 1991. Regulation of Na⁺/Ca²⁺ exchange, an overview. Ann. N.Y. Acad. Sci. 639, 101–111.
- DiPolo, R., Beaugé, L., 2002. MgATP counteract intracellular proton inhibition of the sodium—calcium exchanger in dialyzed squid axons. J. Physiol. (London) 539, 791–803.
- DiPolo, R., Beaugé, L., 2006. Sodium/Calcium exchanger: influence of metabolic regulation on ion carrier interactions. Physiol. Rev. 86, 155–203. DiPolo, R., Beaugé, L., 2008. In the squid axon Na⁺/Ca²⁺ exchanger the state of the
- DiPolo, R., Beaugé, L., 2008. In the squid axon Na⁺/Ca²⁺ exchanger the state of the Ca₁²⁺-regulatory site influences the affinities of the intra- and extracellular transport sites for Na⁺ and Ca²⁺. Pflugers Arch. 456, 623–633.
- DiPolo, R., Berberián, G., Rojas, H., Delgado, D., Beaugé, L., 1997. A novel 13 kDa cytoplasmic soluble protein is required for the nucleotide (MgATP) modulation of the $\rm Na^+/Ca^{2+}$ exchange in squid nerve fibers. FEBS Lett. 401, 6–10.
- DiPolo, R., Berberián, G., Beaugé, L., 2004. Phosphoarginine regulation of the squid nerve Na⁺/Ca²⁺ exchanger: metabolic pathway and exchanger-ligand interactions different from those seen with ATP. J. Physiol. (London) 554, 387–401.
- Doering, A.E., Lederer, W.J., 1993. The mechanism by which cytoplasmic protons inhibit the sodium—calcium exchanger in guinea pig heart cells. J. Physiol. 466, 481–499.
- Doering, A.E., Lederer, W.J., 1994. The action of Na⁺ as a cofactor in the inhibition by cytoplasmic protons of the cardiac Na⁺/Ca²⁺ exchanger in the guinea pig. J. Physiol. 480, 9–20.
- Doering, A.E., Eisner, D.A., Lederer, W.J., 1996. Cardiac Na⁺/Ca²⁺ exchange and pH. Ann. N.Y. Acad. Sci. 779, 182–198.
- Eisner, D., Richards, D.E., 1980. The interaction of potassium ions and ATP on the sodium pump of resealed red cells ghosts. J. Physiol. 319, 403–418.
- Forcato, D., Posada, V., Beaugé, L., Berberián, G., 2010. Optimal metabolic regulation of the mammalian heart Na⁺/Ca²⁺ exchanger requires a special arrangement with a PtdIns(4)-5 kinase. Biochem. Biophys. Res. Comm. 402, 147–152.
- Formisano, L., Saggese, M., Secondo, A., Sirabella, R., Vito, P., Valsecchi, V., Molinaro, P., Di Renzo, G., Annunziato, L., 2008. The two isoforms of the Na⁺/Ca²⁺ exchanger, NCX1 and NCX3, constitute novel additional targets for the prosurvival action of Akt/protein kinase B pathway. Mol. Pharmacol. 73, 727–737.
- Fujioka, Y., Hiroe, K., Matsuoka, S., 2000. Regulation kinetics of Na⁺—Ca²⁺ exchange current in guinea-pig ventricular myocites. J. Physiol. (London) 529, 611—623.
- Gericke, E., Smith, E.R., Moore, D.J., Mendelsohn, R., Storch, J., 1997. Adipocyte fatty acid-binding protein: interaction with phospholipid membranes and thermal stability studied by FT-IR spectroscopy. Biochemistry 36, 8311–8317.
- Gomez, D.,P., Nasi, E., 2005. A direct signaling role of phosphatidylinositol 4,5-biphosphate (PIP2) in the visual excitation process of microvillar receptors. J. Biol. Chem. 280, 16784–16789.

- Haase, A., Hartung, K., 2009. Pre-steady state kinetics of Ba²⁺-Ca²⁺ exchange reveals a second electrogenic step involved ion Ca²⁺ translocation by the exchanger. Biophys. J. 96, 4571–4580.
- Haase, A., Wood, P.G., Pintschovius, V., Bamberg, E., Hartung, K., 2007. Time resolved kinetics of the guinea pig Na⁺–Ca²⁺ exchanger (NCX1) expressed in *Xenopus* oocytes: voltage and Ca²⁺ dependence of pre-steady state current investigated by photolytic Ca²⁺ concentration jumps. Pflugers Arch. 454, 1031–1042.
- Haworth, R.A., Biggs, A.V., 1997. Effect of ATP depletion on kinetics of Na⁺/Ca²⁺ exchange-mediated Ca influx in Na-loaded heart cells. J. Mol. Cell. Cardiol. 29, 503-514
- He, Z., Tong, O., Ouednau, B.D., Philipson, K.D., Hilgemann, D.W., 1998, Cloning, expression, and characterization of the squid Na⁺–Ca²⁺ exchanger (NCX-SQ1). I. Gen. Physiol. 111, 857-873.
- Hilge, M., Aelen, J., Perrakis, A., Vuister, G.W., 2007. Structural basis for Ca²⁺ regulation in the Na⁺/Ca²⁺ exchanger. Ann. N.Y. Acad. Sci. 1099, 7–15.
- Hilgemann, D.W., 1990. Regulation and deregulation of cardiac Na⁺/Ca²⁺ exchange in giant excised sarcolemmal membrane patches. Nature 344, 242–245. Hilgemann, D., 1996. The cardiac Na⁺/Ca²⁺ exchanger in giant membrane patches.
- Ann NY Acad Sci 779 136-158
- Hilgemann, D.W., 1997. Cytoplasmic ATP-dependent regulation of ion transporters
- and channels: mechanisms and messengers. Annu. Rev. Physiol. 59, 193–220. Hilgemann, D., Ball, R., 1996. Regulation of cardiac Na⁺/Ca²⁺ exchange and KATP potassium channels by PIP2. Science 273, 956-959.
- Hilgemann, D., Collins, A., Matsuoka, S., 1992a. Steady-state and dynamic properties of cardiac sodium-calcium exchange: secondary modulation by cytoplasmic calcium and ATP. J. Gen. Physiol. 100, 933-961.
- Hilgemann, D., Matsuoka, S., Nagel, G., Collins, A., 1992b. Steady-state and dynamic properties of cardiac sodium-calcium exchange: sodium-dependent inactivation. J. Gen. Physiol. 100, 905-932.
- Holowka, D., Sil, D., Torigoe, C., Baird, B., 2007. Insights into immunoglobulin E receptor
- signaling from structurally defined ligands. Immunol. Rev. 217, 269–279. Hurtado, J., Borges, S., Wilson, M., 2002. Na⁺/Ca²⁺ exchanger controls the gain of Ca²⁺ amplifier in the dendrites of amacrine cells. J. Neurophysiol. 88, 2765–2777.
- Hryshko, L.V., 2002. Tissue-specific modes of Na/Ca exchanger regulation. Ann. N. Y. Acad. Sci. 976, 166-175.
- Iwamoto, T., Pan, Y., Nakamura, T.Y., Wakabayashi, S., Shigekawa, M., 1998. Protein kinase C-dependent regulation of Na^+/Ca^{2+} exchange isoforms NCX1 and NCX3 does not require their direct phosphorylation. Biochemistry (USA) 37, 17230-17238.
- Kauppinen, J.K., Moffatt, D.J., Mantsch, H.H., Cameron, D.G., 1981. Fourier selfdeconvolution: a method for resolving intrinsically overlapped bands. App. Spectrosc. 35, 271-276.
- Matsuda, T.K., Takuma, K., Baba, A., 1997. Na⁺–Ca²⁺ exchange: physiology and pharmacology. Jpn. J. Pharmacol. 74, 1-20.
- Matsuoka, S., Hilgemann, D.W., 1992. Steady-state and dynamic properties of the cardiac sodium-calcium exchange. J. Gen. Physiol. 100, 963-1001.
- Matsuoka, S., Nicoll, D.A., Reilly, R.F., Hilgemann, D.E., Philipson, K.D., 1993. Initial localization of regulatory regions of the cardiac sarcolemmal Na⁺-Ca²⁺ exchanger. Proc. Natl. Acad. Sci. USA 90, 3870-3874.
- Matsuoka, S., Philipson, K., Hielgemann, D., 1996. Multiple functional states of the cardiac Na⁺/Ca²⁺ exchanger. Ann. N.Y. Acad. Sci. 779, 159–181.
- Molinaro, P., Cuomo, O., Pignataro, G., Boscia, F., Sirabella, R., Pannaccione, A., Secondo, A., Scorziello, A., Adornetto, A., Gala, R., Viggiano, D., Sokolow, S.,

- Herchuelz, A., Schurmans, S., Di Renzo, G., Annunziato, L., 2008. Targeted disruption of Na⁺/Ca²⁺ exchanger 3 (NCX3) gene leads to a worsening of ischemic brain damage. J. Neurosci. 28, 1179-1184.
- Murphy, E., Cross, H.R., Steenbergen, C., 2002. Is Na⁺/Ca²⁺ exchange during ischemia and reperfusion beneficial or detrimental? Ann. NY Acad. Sci. 976, 421–430.
- Noble, D., 2002. Simulation of Na/Ca exchange activity during ischemia. Ann. NY Acad. Sci. 976, 431-437.
- Nolan, V., Parduca, M., Monaco, H.L., Maggio, B., Montich, G.G., 2003. Interactions of chicken liver basic fatty acid-binding protein with lipid membranes. Biochim. Biophys. Acta 1611, 98-106.
- Philipson, K.D., Nicoll, A.D., 2000, Sodium-Calcium exchange, A molecular perspective. Ann. Rev. Physiol. 62, 111–133.
- Pulina, M.V., Rizzuto, R., Brini, M., Carafoli, E., 2006. Inhibitory interaction of the plasma membrane Na⁺/Ca²⁺ exchangers with the 14-3-3 Protein. J. Biol. Chem. 281, 19645-19654.
- Raimunda, D., Bollo, M., Beaugé, L., Berberián, G., 2009, Squid nerve Na+/Ca2+ exchanger expressed in Saccharomyces cerevisiae: up-regulation by a phosphorylated cytosolic protein (ReP1-NCXSQ) is identical to that of native exchanger in situ. Cell Calcium 45, 499–508.
- Riedel, M.J., Baczkó, I., Searle, G.J., Webster, N., Matthew Fercho, M., Jones, L., Lang, J., Lytton, J., Dyck, J.R.B., Light, P.E., 2006. Metabolic regulation of sodium—calcium exchange by intracellular acyl CoAs. EMBO J. 25, 4605-4614.
- Romero-Martin, F.J., Guitierrez Martin, Y., Henao, F., Guitierrez-Merino, C., 2003. Fluorescent measurements of steady state peroxynitrite production upon SIN-1 decomposition: NADH versus dihydrodichlorofluorescein and dihydrorhodamine 123. I. Fluorescence 14, 17-22.
- Salinas, R.K., Bruschweiler-Li, L., Eric Johnson, E., Rafael Brüschweiler, R., 2011. Ca²⁺binding alters the inter-domain flexibility between the two cytoplasmic calcium-binding domains in the ${\rm Na}^+/{\rm Ca}^{2+}$ exchanger. J. Biol. Chem. On line Manuscript M111.249268.
- Schulze, D.H., Polumuri, S.K., Gille, T., Ruknudin, A., 2002. Functional regulation of alternatively spliced Na⁺/Ca²⁺ exchanger (NCX1) isoforms. Ann. N. Y. Acad. Sci. 976, 187-196,
- Song, J., Zhang, X.Q., Wang, J., Cheskis, E., Chan, T.O., Feldman, A.M., Tucker, A.L., Cheung JYTucker, A.L., Cheung, J.Y., 2008. Regulation of cardiac myocyte contractility by phospholemman: Na⁺/Ca²⁺ exchange versus Na⁺–K⁺-ATPase. Am. J. Physiol. Heart Circ. Physiol. 295, H1615—H1625.
- Stock, A.M., Robinson, V.L., Goudreau, P.N., 2000. Two-component signal transduction, Annu. Rev. Biochem, 69, 183-215.
- Suh, B.C., Hille, B., 2008. PIP2 is a necessary cofactor for ion channel function: how and why? Annu. Rev. Biophys. 37, 175-195.
- Tanfani, F., Kochan, Z., Swierczynski, J., Zydowo, M.M., Bertoli, E., 1995. Structural properties and thermal stability of human liver and heart fatty acid binding proteins: a Fourier transform IR spectroscopy study. Biopolymers 36, 569-577.
- Therien, A.G., Blostein, R., 2000. Mechanisms of sodium pump regulation. Amer. J. Physiol. Cell Physiol. 279, 541-566.
- Venyaminov, S.Y., Yang, J.T., 1996. Determination of protein secondary structure. In: Fasman, G.D. (Ed.), Circular Dichroism and the Conformational Analysis of Biomolecules. Plenum, New York, pp. 69-107.
- Woody, R.W., Dunker, K., 1996. Aromatic and cystine side-chain circular dichroism. In: Fasman, G.D. (Ed.), Proteins in Circular Dichroism and the Conformational Analysis of Biomolecules. Plenum, New York, pp. 109-157.